AALBORG UNIVERSITY ESBJERG

Evaluation of shear lag in standard H-/I-sections

Ruben Krogh Sørensen

2013

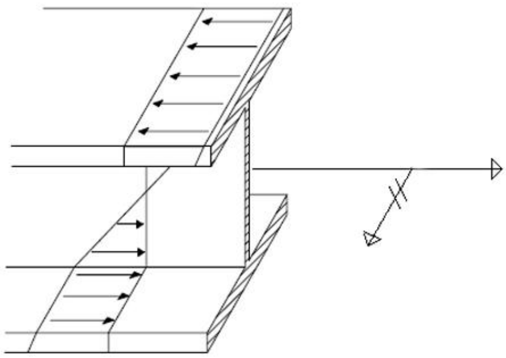

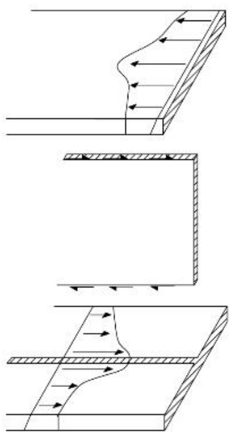

Title: Evaluation of shear lag in standard H-/I-sections

Theme: Master Thesis

Period: February 4th - June 20th 2013

Author: Ruben Krogh Sørensen

Supervisors:
Lars Damkilde (AAU)
Kristian Toft (Ramboll Oil and Gas, Esbjerg)

Number of pages: 64

Number of copies: 5

Attachments: Full report with Appendix including Ansys Workbench files and ROSAP files are enclosed on CD

Ruben Krogh Sørensen

Preface

This thesis has been carried out by Ruben Krogh Sørensen, studying at the 4th semester of: "M.Sc. in Structural and Civil Engineering", at Aalborg University Esbjerg. The report has been produced at the office for Ramboll Oil & Gas in Esbjerg. I will like to give thanks to supervisor professor Lars Damkilde for helping me to understand the shear lag phenomenon and for guidance through the process of writing this thesis. I will like also to give thanks to supervisor Kristian Toft from ROGE for comments to the written text and help with the ROSAP software and thanks to ROGE for providing office space, computer and other office supplies.

Reading guidelines

Through the report references to the appendix is done as App. (x) where the "x" refers to the number in the list of appendices, found right after the table of content. The appendix includes Ansys Workbench files and ROSAP files used through the paper, and some extra material. The appendix is only found on the attached CD in a digitally version.

References to literature and sources is seen in the text as an [x], where the x again refer to the number the literature or source is given in the list of references. This list of references can be found at the end of the report.

Equations are numbered (x.y) where the x refers to chapter and y is a continuous number through each chapter, and a reference in the text to a specific equation could look like e.g. Eq. 2.10.

Figures are numbered continuous through the report. If no reference to another source is seen in the figure caption it is produced by the author.

Abstract

The stress distribution in a transverse loaded I-section beam is different from what is calculated by classical beam theory because of shear lag, and this is the topic for this master thesis. Shear lag provides a stress distribution that is not uniform in an I-section flange, and the mechanism causing this is described. It is described how shear lag is included by reducing the flange width to an "effective width" when the load bearing capacity for a beam is calculated.

In 1924 Th. Von Karman described a theoretical solution for shear lag, which later were referred by Timoshenko and Goodier in their book: *Theory of elasticity*. The solution was for a continuous T-section beam on equidistant supports with an infinite wide top-plate. A theoretical solution for shear lag in beams can be hard and time consuming to find, why a simplified method is suggested in EC3.

The effective width for a beam has been calculated by the use of the theoretical solution referred to by Timoshenko and Goodier, and also for a solution based on a Finite Element Model (FE-Model). The effective width calculated by both methods has been compared.

The shear stresses have been seen to affect the effective width, and it is described how big shear stresses at supports influence the normal stresses and cause a smaller effective width. From another example it is also seen how the effective width is dependent on the shear stiffness of the used material.

The background for how the simplified method include shear lag described in EC3 has been studied, and solutions achieved by this method is compared to solutions calculated from a FE-Model meshed with shell elements.

Inspiration to this thesis came from Ramboll Oil & Gas where interest was raised whether shear lag effects has to be included in standard size I-sections. From EC3 it is not clear whether this is the case for this kind of beams why this has been examined in a simple situation. A part of a structure where shear lag effects has been included according to EC3 has been copied to a FE-Model with shell elements. Here the effect of shear lag has also been calculated. The original structure was assessed with a FE-program using beam elements, where shear lag was included by using the method described in EC3. Results achieved by this method have been compared with results extracted from the shell model. It was found that using the method described in EC3, led to a conservative solution. It was also found that if a beam was fully attached to an adjacent beam, then the propagation of shear lag along the beam would be less than if the beam was calculated as simply supported.

Resumé

Spændingsfordelingen i en tværbelastet I-bjælke er anderledes, end den klassiske bjælke teori beskriver pga. forskydningsdeformationer, hvilket er emnet for dette Master speciale. Forskydningsdeformationer giver en uens spændingsfordeling i en I-bjælkes flanger, og mekanismen som forårsager dette er beskrevet. Det er beskrevet hvordan forskydningsdeformationer er inkluderet ved at reducere flange bredden til en "effektiv bredde" når en bjælkes bæreevne skal beregnes.

I 1924 beskrev Th. von Karman en teoretisk løsning for forskydningsdeformationer, som senere blev refereret af Timoshenko of Goodier i deres bog: Theory of Elasticity. Løsningen var for en kontinuert T-bjælke på ækvidistante understøtninger, med en uendelig bred top plade. En teoretisk løsning for forskydningsdeformationer i bjælker kan være vanskelig og tidskrævende at finde, hvorfor en forenklet metode er anvist i EC3.

Den effektive bredde for en bjælke er blevet beregnet vha. den teoretiske metode som Timoshenko og Goodier referer til, og også for en løsning baseret på en FE-Model. Den beregnede effektive bredde fra de to metoder er blevet sammenlignet.

Det vises hvordan den effektive bredde bliver påvirket af forskydnings spændinger, og det er beskrevet hvordan store forskydnings spændinger ved understøtningerne påvirker normal spændingerne og dermed giver en mindre effektive bredde. Fra et andet eksempel er det også vist, hvordan den effektive bredde er afhængig af forskydningsstivheden af det anvendte materiale.

Baggrunden for, hvordan den forenklede metode fra EC3 inkluderer forskydningsdeformationer er undersøgt, og løsninger opnået ved denne metode er sammenlignet med løsninger beregnet fra en FE-Model opdelt i skal elementer.

Inspiration til dette speciale kom fra Rambøll Olie & Gas, hvor interesse blev rejst om, hvorvidt forskydnings deformationer skal inkluderes i I-bjælker i standart størrelse. I EC3 er det ikke tydeligt hvorvidt dette er tilfældet for denne slags bjælker, hvorfor dette er blevet undersøgt i en simpel situation. En part af en struktur hvor effekten af forskydningsdeformationer er blevet inkluderet i henhold til EC3, er blevet kopieret til en FE-Model opdelt i skal elementer. I denne model blev effekten af forskydnings deformationer også beregnet. Den oprindelige struktur blev beregnet med et FE-program som anvender bjælke elementer, og dermed inkluderet forskydningsdeformationer vha. metoden beskrevet i EC3. Resultater opnået ved EC3 metoden er blevet sammenlignet med resultater beregnet fra skal modellen. Det kunne ses, at metoden beskrevet i EC3 førte til en konservativ løsning. Det kunne også ses, at hvis en bjælke var sammenkoblet med en tilstødende bjælke, så blev udbredelsen af forskydningsdeformationer langs bjælken mindre end hvis bjælken var simpelt understøttet.

Table of content

Appendices

App (1): Normal stress distribution in T-section according to Th. von Karman

App (2): Calculation of principal stresses and angles by Mohr's circle

App (3): Ansys Workbench files for T-section beam (section 2.2 in the report)

App (4): Ansys Workbench files for 3 span I-section beam (section 4.1 in the report)

App (5): ROSA – STRECH input and output files (section 5.1.1 in the report)

App (6): ROSA – STRECH input and output files for lifeboat structure, and drawings (section 5.2 in the report)

App (7): Ansys Workbench files for lifeboat structure (section 5.3 in the report)

Abbreviations

App.	Appendix
EC3	A reference to the following codes: DS/EN 1993-1-1 and DS/EN 1993-1-5 and EN 1993 DK NA
Eq.	Equation
ROG	Ramboll Oil & Gas
ROSAP	Ramboll Offshore Structural Analysis Program Package
ROSA	Ramboll Offshore Structural Analysis (part of ROSAP)
STRECH	Member stress analysis (part of ROSAP)
GLORIA	Interactive graphical display (part of ROSAP)

1. Introduction

Offshore topside structures are made of large horizontal steel girders and vertical pipe-sections. With the introduction of DS/EN 1993-1-1[1] and DS/EN 1993-1-5[2], beams exposed to a transverse load, has to be checked for shear deformations causing a stress distribution over the cross section that is not uniform, this is termed "shear lag". A note in [1] states that in rolled sections and welded sections with similar dimensions the effects of shear lag *may* be neglected. As the Eurocode not clearly states if the effect of shear lag should be included in hot rolled I-sections and sections with similar dimensions, this will be examined in this thesis.

Following is given a short introduction of the mechanism giving shear lag in I-sections.

1.1. Shear lag

When a beam is exposed to a transverse load the classical beam theory provides a uniform stress distribution of the longitudinal stresses in the flanges as illustrated in Figure 1.

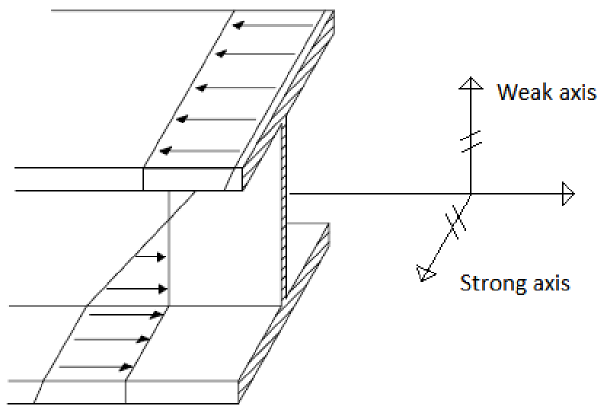

Figure 1: Uniform normal stress from bending moment according to classical beam theory

This may however not be how the stresses are distributed in reality. The longitudinal stresses from a bending moment around the strong axis are transmitted to the flanges through shear deformations in the junction between the web and the flange as illustrated in Figure 2.

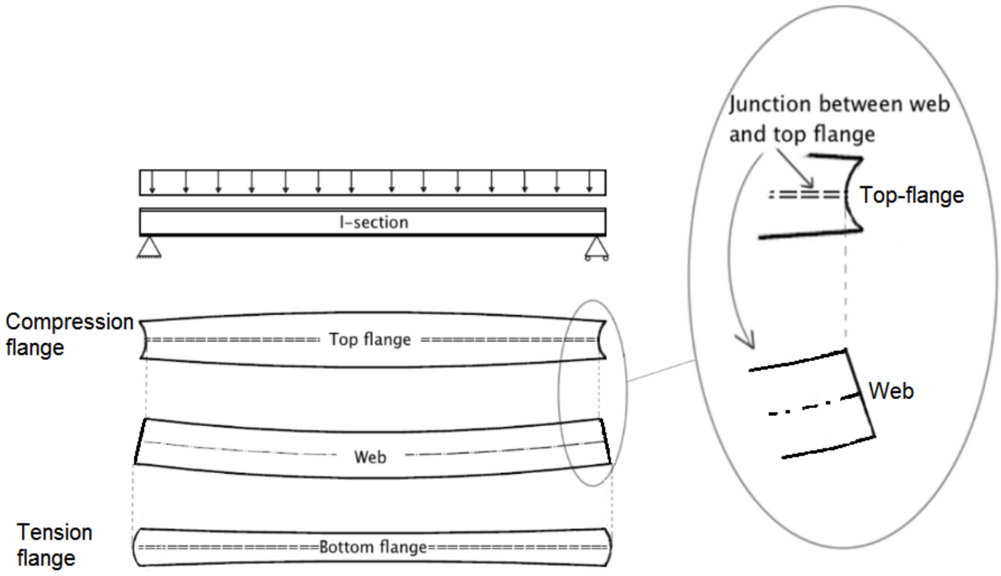

Figure 2: Mechanism in I-section beam when exposed to bending around strong axis and simply supported, deformation is exaggerated

The mechanism is sketched in Figure 2 for a simply supported transverse loaded I-section beam. When the beam is bending, the top flange will be compressed at the joint between flange and web, and the bottom flange will be stretched at the joint with the web. This leads to a deformation pattern in the joint between web and flanges at the beam-ends as seen in Figure 2.

As the top flange experience compression in the longitudinal direction when loaded as seen in Figure 2, the flange becomes shorter, and due to Poisson's ratio it becomes wider. The opposite apply for the bottom flange.

If the flanges are wide, the deformation pattern will cause a non-uniform distribution of the longitudinal stresses caused by a lag in activating the furthest fibers in the flanges. This causes the parts of the flanges that are farthest away from the web to not take its full share in resisting the normal stress, and the beam will act weaker than classical beam theory indicates. This situation with a non-uniform stress distribution in a flange is termed "shear lag" and illustrated in Figure 3.

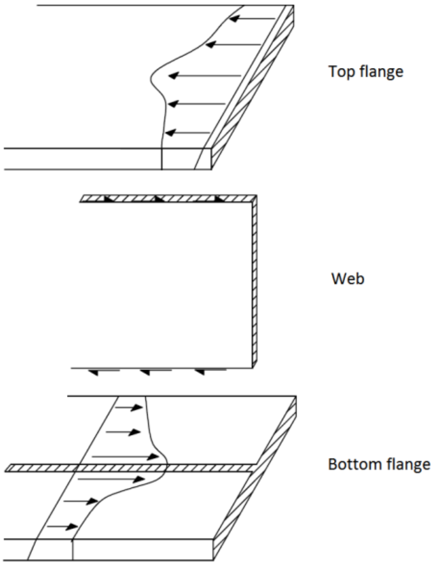

Figure 3: Not uniform normal stress in flanges from bending moment

In [1] shear lag is included by calculation of a reduced flange width. When reduction is caused by shear lag the effective width is termed "effective^{s} width", which is not to be confused by reduction of the width caused by plate buckling, termed "effective^{p} width". Shear lag is relevant both for flanges in tension and in compression. Plate buckling on the other hand is only relevant for flanges in compression. Both effects should be considered when the cross sectional properties are calculated, but in the present study focus will only be on effects caused by shear lag why the $^{"s"}$ in effective width not will be used.

When the flange width is reduced to an effective width, the classical beam theory gives the correct maximum stresses, and the correct load bearing capacity of the girder. In Figure 4 is illustrated the reduced flange width and the uniform axial stress distribution calculated by classical beam theory.

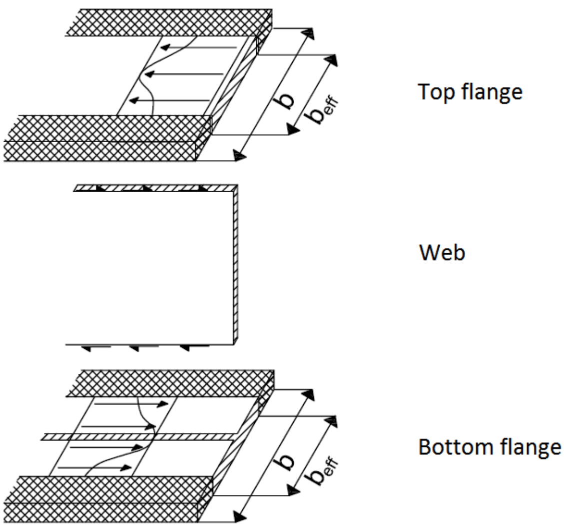

Figure 4: Flange width 'b' reduced to an effective width 'b_{eff}' and a uniform stress distribution calculated by classical beam theory can be used to determine the maximum stresses in the flanges

Formulas in [2] to calculate the effective width is based on the situation seen in Figure 5. The assumption is a simply supported continuous beam. This is similar to the situation seen in Figure 2 and will cause the shear lag phenomenon to be introduced. However this is often not the case for a beam on e.g. an offshore topside structure. Here the flange ends will often be welded to adjacent members, and the propagation of shear lag would be different from what is described in [2]. This raises two questions:

- What has influence on the amount of shear lag?
- What happens with respect to shear lag when a beam is welded to an adjacent member?

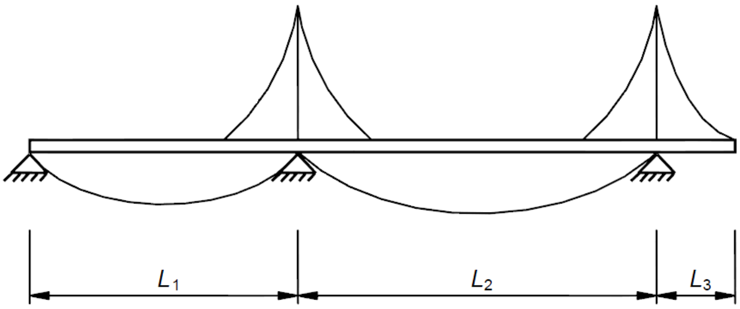

Figure 5: Describing the support and moment giving basis for the formulas for effective width in [1]

At Ramboll Oil & Gas (ROG), shear lag is always included when the load bearing capacity of girders on offshore topside structures are checked. The primary used software includes the effects of shear lag by the formulas from [2] as a default. But a note in section 5.2.1 in [1] states: "*For rolled sections and welded sections with similar dimensions shear lag effects may be neglected*." This raises two questions:

- Does the effect of shear lag have to be included when a structure is designed with standard section I-beams?
- Is the primary used member stress analysis software at ROG making too conservative calculations when shear lag is included?

These questions will be examined and answered through this Master's thesis.

2. Shear lag theoretically and by Finite Element Method

In section 1.1 a suggestion upon the mechanism causing shear lag in a simply supported I-section beam is given, in this section this will be further analyzed from an analytical point of view and also the problem will be looked upon in a Finite Element Model. The FEM analysis will be performed in Ansys Workbench.

2.1. Theoretical approach to effective width

A theoretical solution to the problem, with effective width, has been described by many. In 1924 Th. von Karman [3] developed a solution on the basis of a stress function. His method has been further developed and is referred to by Timoshenko and Goodier in their book: Theory of Elasticity [4]. In his solution Karman analyzed an infinitely long continuous beam on equidistant supports. The span length is *2l* and the beam is reinforced by a thin plate, which is considered of infinite width. All spans are loaded symmetrically and equally. The beam is sketched in Figure 6. No flexural stiffness of the top-plate is considered, and the stresses in the plate are considered only two-dimensional.

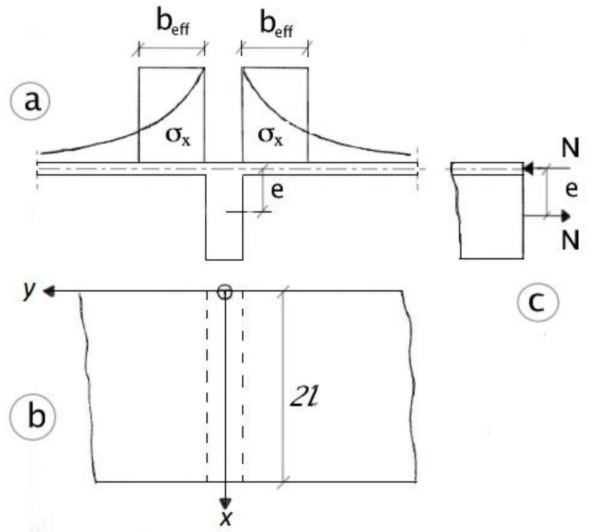

Figure 6: The effective width [4]

The stress distribution in the plate can be found by solving the compatibility equation seen below.

$$\frac{\partial^4 F}{\partial x^4} + 2\frac{\partial^4 F}{\partial x^2 \partial y^2} + \frac{\partial^4 F}{\partial y^4} = 0 \qquad 2.1$$

Where *F* is the stress function, also known as Airy's stress function:

$$F = \sum_{n=1}^{\infty} \left[A_n e^{\frac{-n\pi y}{l}} + B_n \left(1 + \frac{n\pi y}{l}\right) e^{\frac{-n\pi y}{l}} \right] \cos\frac{n\pi x}{l} \qquad 2.2$$

By means of the minimal strain energy the constants A_n and B_n are determined. A situation where the bending moment diagram is a cosine line is chosen:

$$M = M_1 \cos\frac{\pi x}{l} \tag{2.3}$$

In Eq. 2.2 n is taken equal to 1, and A_1 and B_1 are determined:

$$A_1 = \frac{lX_1}{2\pi h} \tag{2.4}$$

$$B_1 = -\frac{(1+\nu)lX_1}{4\pi h} \tag{2.5}$$

And X_1 is:

$$X_1 = -\frac{M_1}{e}\frac{1}{1+\frac{I}{Ae^2}+\frac{n\pi I}{he^2 l}\cdot\frac{3+2\nu-\nu^2}{4}} \tag{2.6}$$

Where:

h	is the thickness of the top-plate.
e	is the distance seen in Figure 6 and
M_1	is the maximum bending moment from Eq. 2.3.

The normal stress in the flange is then given by:

$$\sigma_x = \frac{\partial^2 F}{\partial y^2} \tag{2.7}$$

The effective width "$2b_{eff}$" of a T-beam can be determined from:

$$2b_{eff} = \frac{4l}{\pi(3+2\nu-\nu^2)} \tag{2.8}$$

And with $\nu = 0.3$ then the effective width of the flange will be approximately 18% of the span.

$$2b_{eff} = 0.181(2l) \tag{2.9}$$

2.1.1. Example using the theoretical solution

Using the above expression to calculate the effective width in a T-section beam with a span length of *2 m* and a uniform load of $q = 200\ kN/m$ the maximum moment in a simply supported beam is $M_{max} = 100\ kNm$ corresponding to M_1 in Eq. 2.3. The situation is illustrated below.

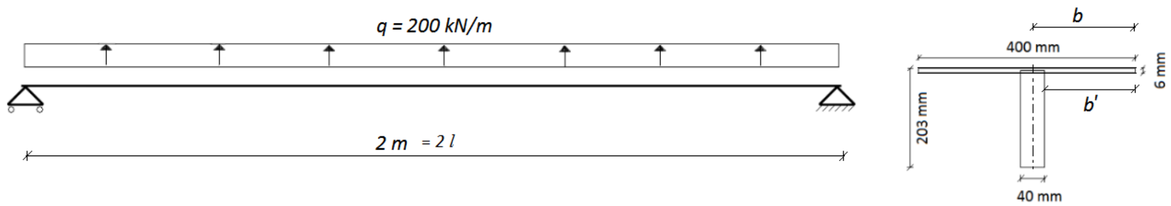

Figure 7: Eq. 2.9 will be used to calculate the effective width for the top-plate of this beam

The normal stress distribution in the top plate by Eq. 2.7 looking only at the positive y-axis, will then be as seen below (the calculation is done in Maple and can be seen in App. (1)). Using the geometry seen in Figure 7 the effective width of the top plate according to Eq. 2.9 will then be: $0.181 \cdot 2\ m = 362mm$.

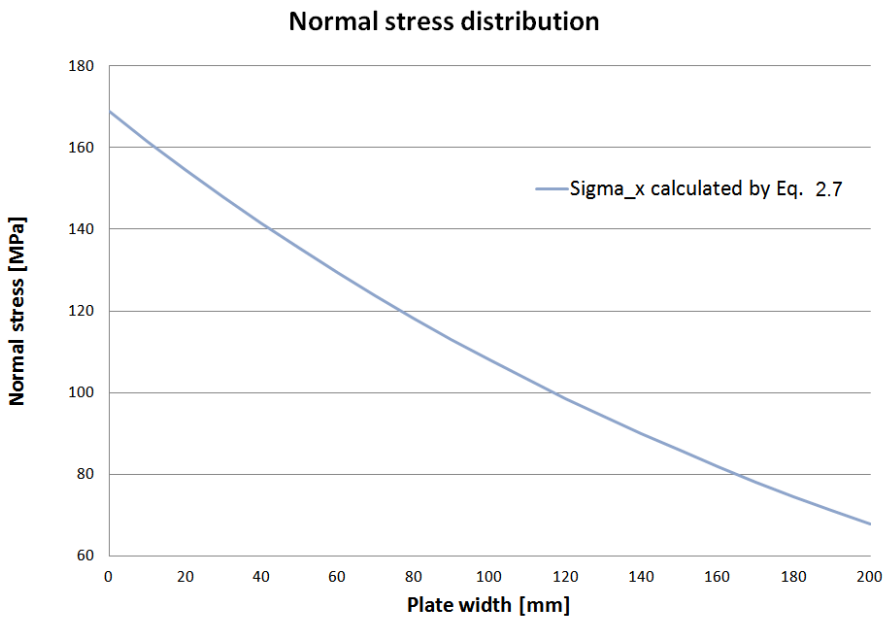

Figure 8: Normal stress distributions in the top plate of a T-beam, only looking at the positive y-axis as described in Figure 6

When the normal stresses in the beam not are uniformly distributed but higher close to the web than at a distance from the web, it will cause the deflections and the stresses of the beam to be higher than classical theory predicts and because of this it can be necessary to design with shorter spans and bigger dimensions to compensate for the effects of the non-uniform stress distribution.

2.2. FEM approach to effective width

In this section shear lag will be looked at in a FE-Model and the effective width will be compared to what was found in the former section where reference was done to an analytical solution.

A FEM approach is the most popular method to simulate the physical behavior of a structure, but still it is an approximate solution, and the solution greatly depends on how the structure is modeled, meshed and how the boundary conditions are applied.

A T-section beam is modeled in Design Modeler in Ansys Workbench. The beam is modeled with the dimensions, load and supports as described in the figures below. The model is supported at the beam-ends in the z-direction. The support is applied to all end-nodes of the web as seen with yellow below. Week springs have been added in Ansys for the structure not to experience rigid body motion.

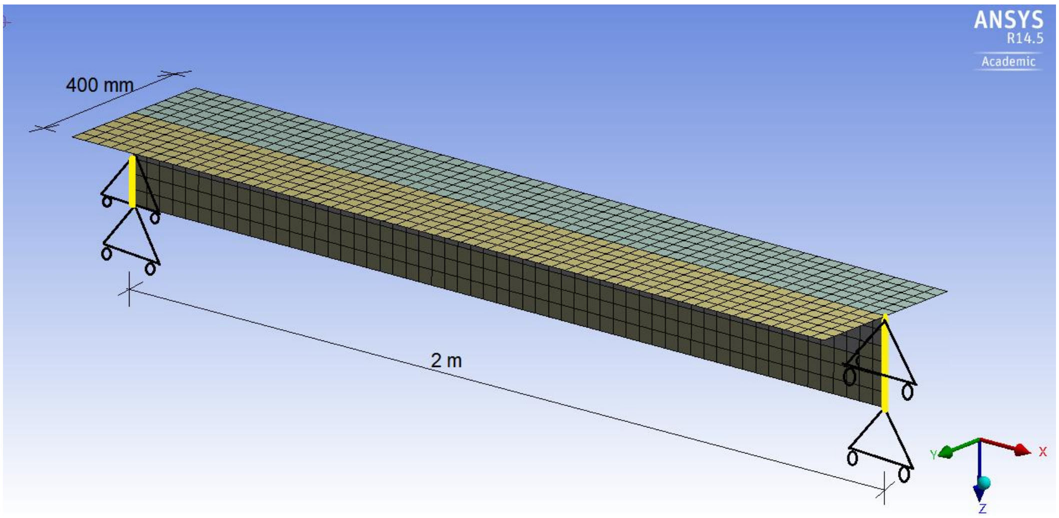

Figure 9: Modeled beam in Ansys, the model is supported in all end nodes in the web (see yellow line) with a displacement support = 0 in the z-direction

The load is imposed as a line load at the centre of mass of the web as seen below.

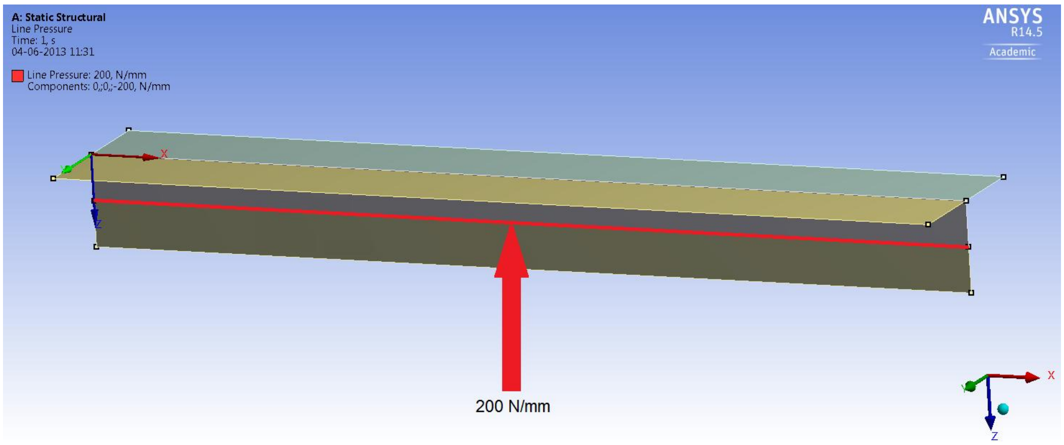

Figure 10: Load in Ansys applied to the center of mass of the web

The modeled beam is meshed with shell elements and given a thickness from the mid-surface of the elements. In the joint between web and flange the elements overlap as seen below. This causes the stresses in the joint to be inaccurate, and when the effective width is calculated, only stresses from outside this overlap is used. This applies for all the Ansys models used in this thesis.

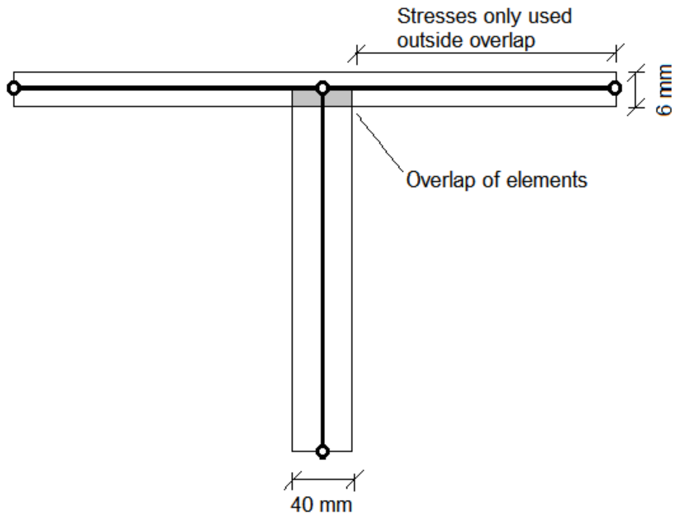

Figure 11: Overlap of shell elements in Ansys, giving inaccurate stresses at the joint

In Ansys Workbench both a four-node quadrilateral shell element (SHELL181), and an eight-node shell element (SHELL281) is available. The shell elements have six degrees of freedom at each node: three translations and three rotations. The model has been tried meshed with both types of elements. To determine which element to use, a convergence study on number of nodes and maximum displacement has been performed, and can be seen in Figure 12.

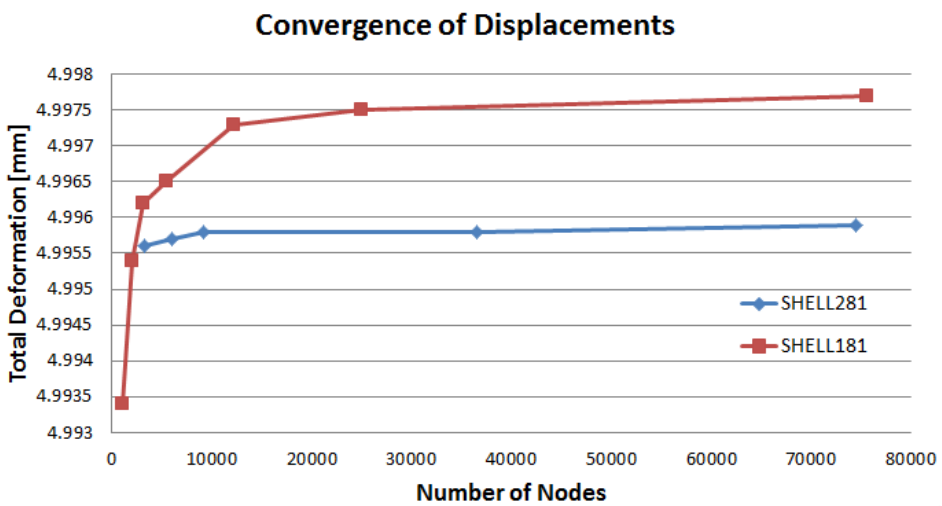

Figure 12: Quadrilateral elements (SHELL281) with eight nodes converge faster than quadrilateral element with four nodes (SHELL181)

Ansys Workbench also has an option called: "Structural Error", which is the difference between strain energy calculated from the element stresses (unaveraged stresses in Ansys), and strain energy calculated from the nodal stresses (averaged stresses in Ansys). This value indicates how well the global mesh adequacy is, and generally a low value is wanted. In Figure 13 the structural error is seen for increasing number of nodes for the two element types.

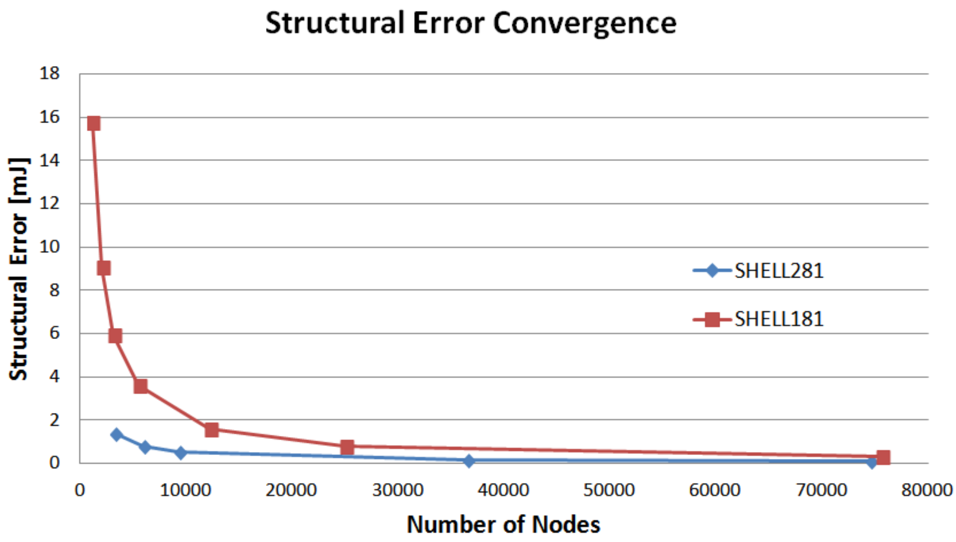

Figure 13: Convergence of the structural error for the two element types

From Figure 12 it is seen that the eight node quadrilateral element (SHELL281) performs best with respect to convergence of displacement. With respect to the value of structural error seen in Figure 13 it is seen that SHELL281 has a much smaller error, making this element the best choice of the two. A maximum element size of 7 mm giving 74533 nodes with SHELL281 and a structural error of 0.0828 [mJ] is chosen for the model.

2.2.1. Example using FEM solution

After a solution has been found for the numerical model, the effective width will be calculated.

In Figure 14 the deformation and the normal stress distribution of the Ansys model is seen.

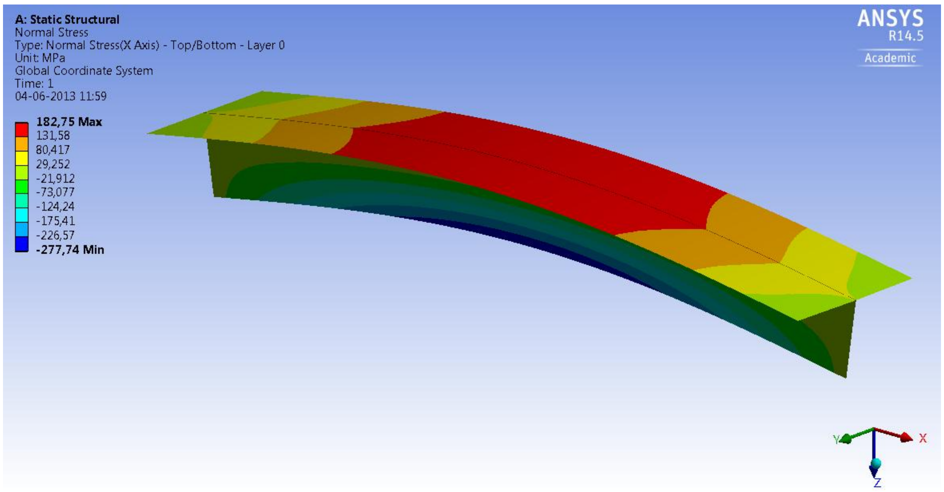

Figure 14: Normal stress distribution of FE-Model in the x-direction, maximum value: 182.75 MPa, the model has a directional deformation in the negative z-direction of 4.996 mm. The model is meshed with shell elements with 8 nodes

In Figure 14 the maximum tension stress is colored with red, corresponding to a uniform load in the negative z-direction. From the distribution of the normal stresses a factor β (a flange width reduction factor) has be calculated by Eq. 2.10.

$$\beta = \frac{\int_0^{b'} \sigma_x dy}{\sigma_{x,max}} \qquad 2.10$$

And the effective width is then calculated by Eq. 2.11.

$$b_{eff} = \beta \cdot b \qquad 2.11$$

In Eq. 2.11 b is half the gross width of the flange, and b' in Eq. 2.10 is the net flange out-stand without the web-flange overlap, as seen in Figure 15. The normal stress distribution in the plate at x-coordinate = 1 m (maximum bending moment) can be seen in Figure 16.

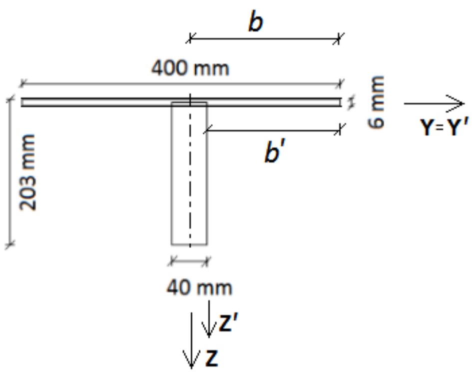

Figure 15: Dimensions of T-section and definition of *b* and *b'*

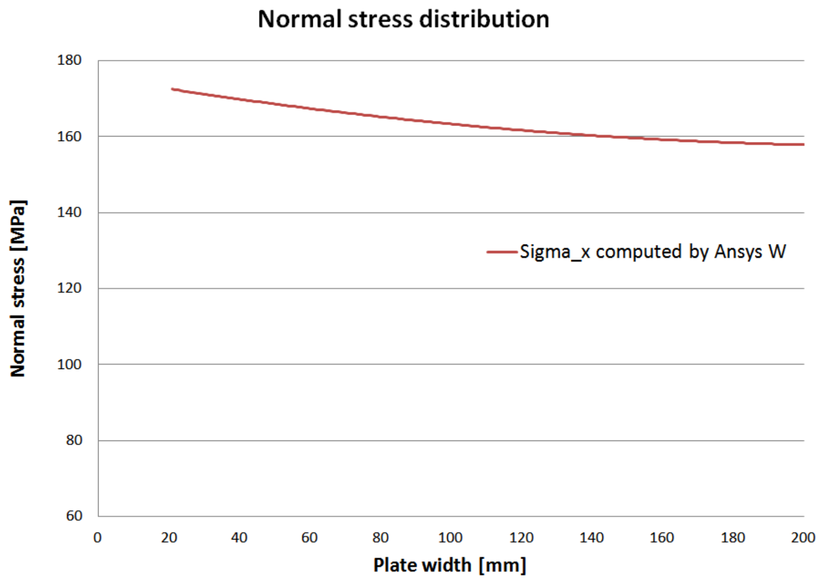

Figure 16: Normal stress distribution in top plate of T-beam, only looking at the positive y-axis at x = 1 m

The effective width of the beam is calculated by Eq. (2.10 and 2.11) 50 mm from the end-support, at *L*¼ and at *L*½, and the width is assumed linear between the calculated points. The result can be seen in Figure 17. The effective width is calculated 50 mm from the end support to get a positive value, the reason for this is explained below.

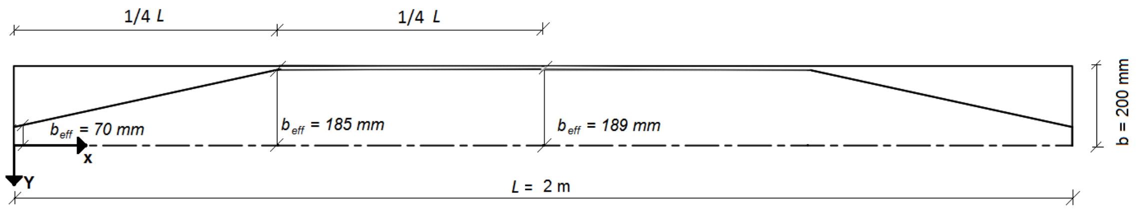

Figure 17: Effective width of flange calculated from normal stress distribution in FE-Model

At the middle of the beam the effective width of the top plate is 4 % wider when calculated from the FE-Model than when calculated by the theoretical method from section 2.1.1.

The small effective width at the supports of the beam has to be explained by looking at the curve for the shear force, see Figure 18.

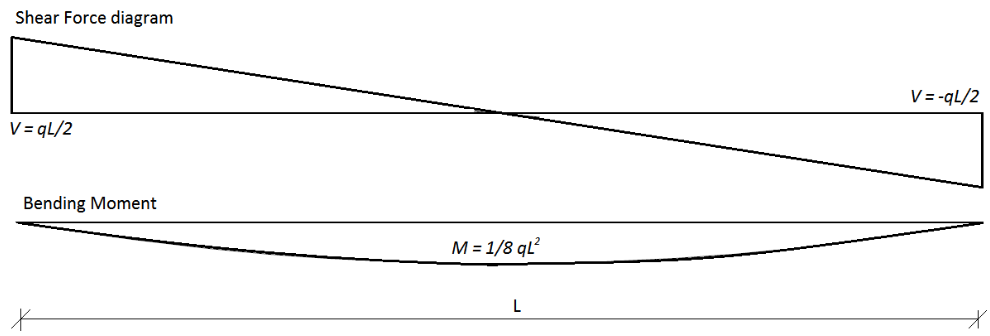

Figure 18: Shear force and bending moment diagram

The large shear forces at the beam-ends are caused by reaction forces from the support. The bending moment is zero at the end of the beam, and will not cause stresses in the plate, but the large shear forces at the beam-end will cause stresses in the axial direction of the thin top plate (plane stress is assumed). The shear stress propagation in a t-section will be as seen below.

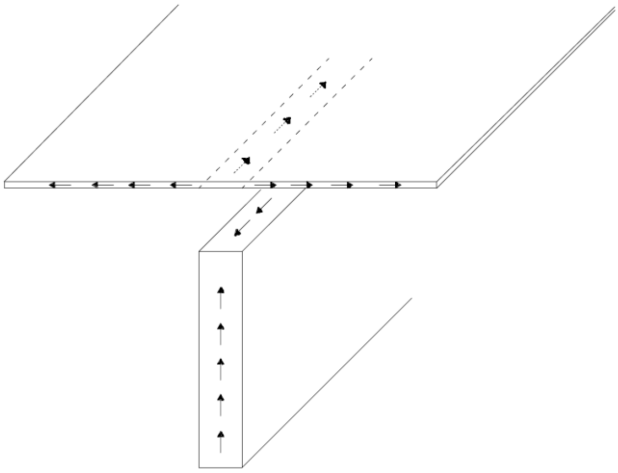

Figure 19: Shear stress distribution in the T-section beam

The plane stress assumption can be verified by checking the normal stress in z-direction in the top-plate in the FE-Model seen below.

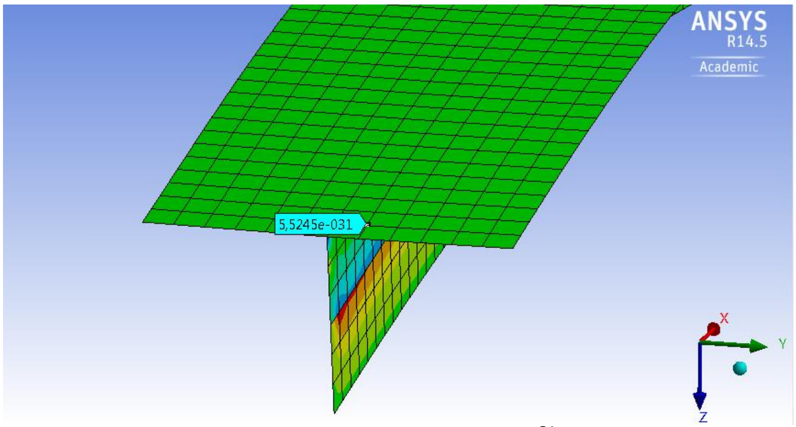

Figure 20: The z-direction normal stress is $5.5 \cdot 10^{-31}$ or almost equal to 0

Looking at the same point as in Figure 20 the normal stresses in x- and y-direction and the shear stresses are:

σ_x:	*23.2 MPa*
σ_y:	*51.0 MPa*
τ_{xy}:	*48.6 MPa*

The direction and size of the principal stresses and of the maximum shear stress in a plane stress situation can be found from the above normal and shear stresses by the use of Mohr's circle. The calculation done by Mohr's circle can be found in App. (2). The maximum principal stress is *87.55 MPa* and found when the x-axis is rotated 53^0 in the clockwise direction as also seen on the vector plot from Ansys.

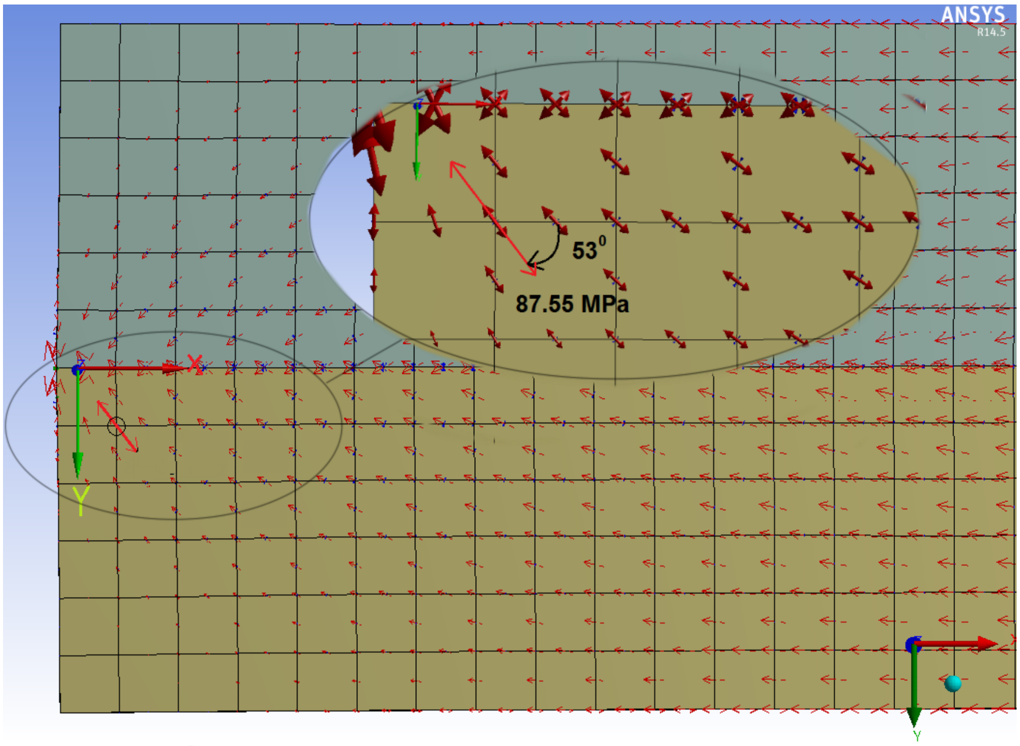

Figure 21: Direction for maximum principal stress in top-plate

The maximum shear stress is *50.55 MPa* and found when the x-axis is rotated 8^0 in the clockwise direction. As shear stresses are working in pairs of opposite directions and $\tau_{xy} = \tau_{yx}$ it is seen that the maximum shear stresses are almost following the global x- y-directions, for the looked at point.

The large shear force at the beam-end causes shear stresses to develop in the web and in the plate. The large shear stresses changes the direction of the principal stresses and results in a small effective width at the beam-end. Shear stresses working on an infinitesimal element leads to a change in the direction of the principal stresses, this can be understood from the figure below.

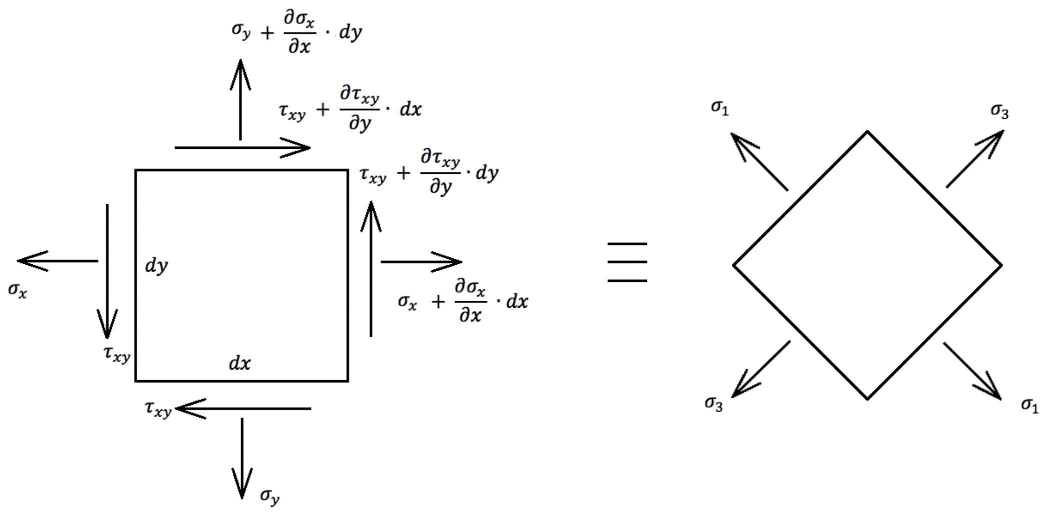

Figure 22: The shear stresses change the direction of the principal stresses on an infinitesimal element

As there is no moment at the beam-end, the principal stresses are caused by the shear stresses, and the angle between shear stress and principal stress is 45^0, then the principal stresses are close to a 45^0 angle to the beam axis. The direction and the distribution of shear stresses in the beam-end can be seen in Figure 23 [5]. Also as the shear stresses approaches zero at the plate edge, the principal stresses vanish here and this part of the plate is not activated.

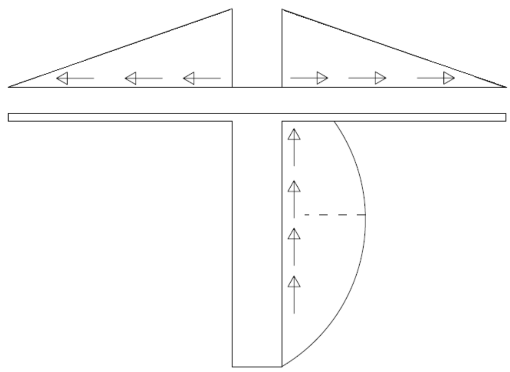

Figure 23: Shear stress distribution in T-section

On the vector plot in Figure 21 the size of the arrows indicate the size of the principal stresses, and as it can be seen the principal stresses approaches zero at the plate edge over the support, indicating that these parts of the beam does not take it's share in carrying the load. The Ansys Workbench files used in this section can be found in App. (3).

The effective width also depends on the ratio E/G (E-modulus / Shear modulus) where: $G = \frac{E}{2(1+\nu)}$ for a homogeneous isotropic material. This ratio expresses the relationship between compression stiffness and the shear stiffness. By the definition of G it can be seen that ν (Poisson's ratio) has an influence [6]. If Poisson's ratio were bigger it would decrease the shear stiffness and the effects of shear lag would be bigger. The values for E, G and ν do not vary much for steel but for an anisotropic material as wood the effects of shear lag can be much bigger.

The E-modulus for steel is often taken as:
$E = 210000\ N/mm^2$ which is the advised value in [1], but it can be different in other standards. If the calculation is performed according to ISO Standards, then $E = 205000\ N/mm^2$ should be used.

Poisson's ratio for steel is *0.3* expressing the ratio between axial strain and transverse strain.

This provide a Shear modulus of $\approx 81000\ N/mm^2$ when performing calculations according to [1] and a little lower when using ISO Standards.

As an example a reference is done to an old Danish specification for wooden structures (SBI-Anvisning 135) [6]. When looking at a wooden plate member with a cross section as seen below, the normal stresses between the webs is described to be smaller because of the low shear modulus.

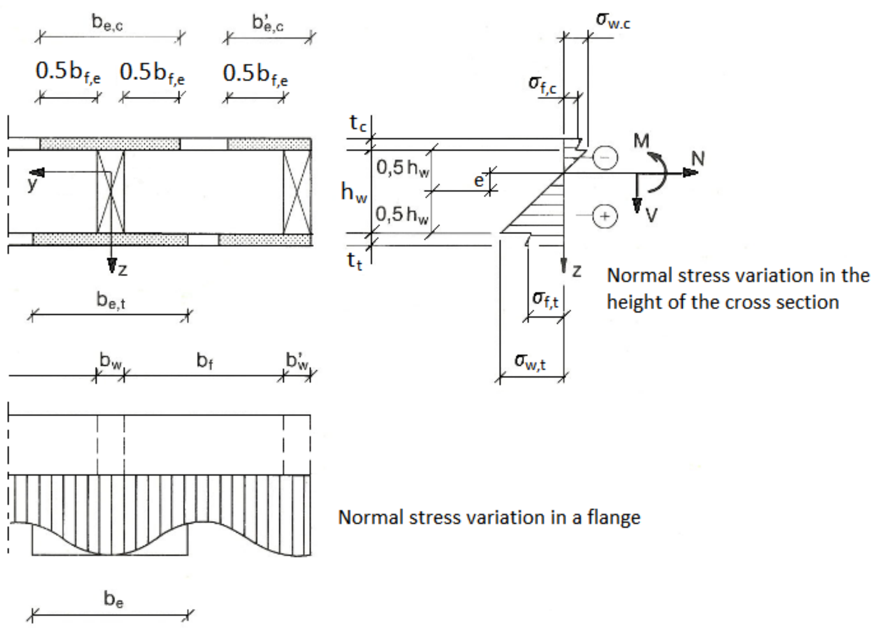

Figure 24: Normal stress variation in a wooden plate member, where: b_e is effective width for compression (index c) and tension (index t), *t* is thickness, *h* is height, $b_{f,e}$ is the effective flange outstand and index *w* is for the web [6]

In [6] directions are given for calculating the effective width for two types of plates: chipboards and plywood sheets, in a compound plate beam as seen in Figure 24. The effective width is depending on the value of the shear modulus, where chipboards can have a shear modulus almost twice as large as plywood. Below is seen a table from [6] with the effective width relative to the span length *l* or the distance between pints of zero bending moment, whatever is smallest. As seen chipboards can have an effective width twice the effective width of plywood sheets, caused by the higher shear modulus.

Table 1: Effective width $b_{f,e}$ for wooden compound beams with thin flanges [6]

Flange		$b_{f,e}$	b_{max}
Plywood	Fibers along web	$0.1 \cdot l$	$20\ t_f$
	Fibers normal to web	$0.1 \cdot l$	$25\ t_f$
Chip board		$0.2 \cdot l$	$30\ t_f$

In Table 1 the b_{max} value only applies for the compression flange and t_f is the thickness of the flange.

3. Background for effective width in EC3

In this section focus is only on how the effective width is calculated in Eurocode 3 (EC3).

EC3 applies for steel constructions in both buildings and other civil engineering structures. Clause 1.5.7 in EN 1993-1-1[1] states that shear deformations are taken into account in wide flanged beams by using a reduced flange width. When the resistance of a cross-section is calculated, clause 6.2.1 in [1] refers to EN 1993-1-5 [2].

In this thesis focus is isolated on shear lag and the effective flange width. In [2] a *"s"* in *effective^{s}* indicates reduction caused by shear lag, but it will not be used here as only shear lag is the topic, and only section 3 in [2] is of interest. "Commentary and worked examples to EN 1993-1-5" [7] is a general reference to the method for calculating the effective width described in this section. Also a paper written by G. Sedlacek: "A Simplified Method for the Determination of the Effective Width Due to Shear Lag Effects" [8] has been used as inspiration to understand the principles behind the method to calculate effective width in [2].

The calculation of the effective width will be held in the elastic range in this section.

Chapter 3 in [2] presents a simple way to calculate the effective width in a simply supported multiple span beam. The effective width (b_{eff}), or a reduced flange width, is calculated by multiplying a factor β to the gross width of the flange outstand b_0.

$$b_{eff} = \beta \cdot b_0 \tag{3.1}$$

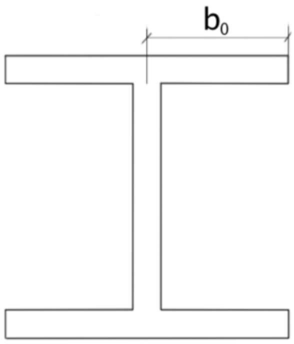

Figure 25: Flange outstand b_0 of an I-section

The principle for calculating β described in [2] is based upon the compatibility condition as also described about the theoretical solution in section 2.1. This requires that the displacements are continuous and single-valued functions of position [9]. In Eq. 3.2 the compatibility is expressed in strains. When the strains are replaced by stresses and the stresses are replaced by Airy's stress function the compatibility equation is seen in Eq. 2.1 [10], and as mentioned in section 2.1 this solution is valid only for a plane problem.

$$\frac{\partial^2 \varepsilon_x}{\partial y^2} - \frac{\partial^2 \gamma}{\partial x \partial y} + \frac{\partial^2 \varepsilon_y}{\partial x^2} = 0 \tag{3.2}$$

Where:

ε_x is the longitudinal strain
ε_y is the transverse strain
γ is the share strain

The solution is simplified by assuming no deformation in the transverse direction $\varepsilon_y = 0$ and only the deformations in the longitudinal direction needs to be considered. With this assumption Eq. 3.2 reads:

$$\frac{\partial \varepsilon_x}{\partial y} - \frac{\partial \gamma}{\partial \mathrm{x}} = 0 \qquad 3.3$$

Warping functions, which describe the shear deformations in the cross section are formulated, see [7], and a general formulation that describes β is sought for. For this purpose the shape of the bending moment curve needs to be considered. Looking at a continuous beam with uniform load the bending moment curve could look like described below.

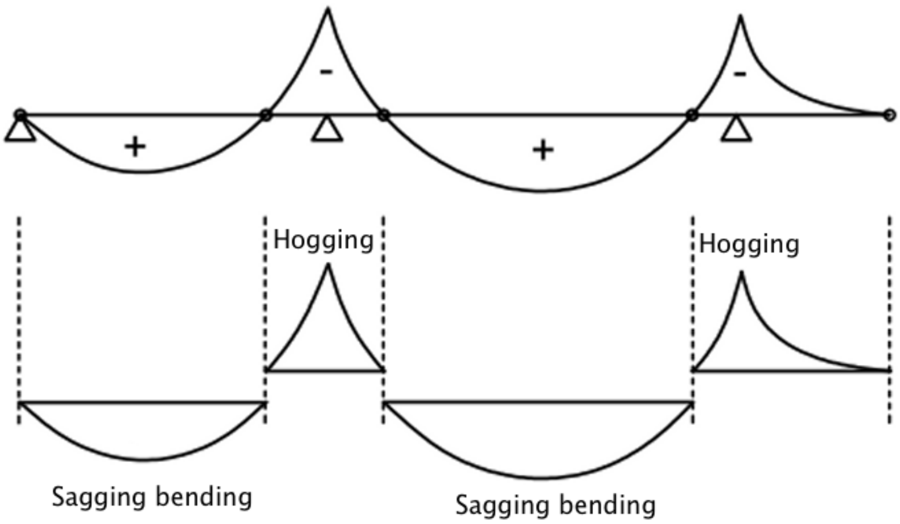

Figure 26: Bending moment curve of continuous simply supported beam with uniform load [8]

By separating the moment curve into individual parts, a formula for β can be based on the shape of the bending moment curve, as for a series of simply supported beams. The shape of the moment curve can be defined by a shape parameter ψ, defined by the maximum bending moment and the convexity of the moment curve, see below.

$$\psi = 4\frac{\Delta M}{M_{max}} \qquad 3.4$$

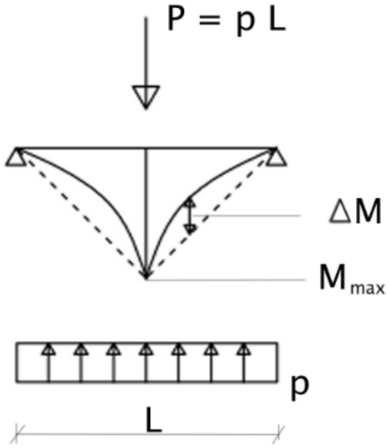

Figure 27: Statically system defining the shape parameter for the bending moment curve, see Eq. 3.4

The shape parameter can now be used to describe the individual parts of the bending moment curve seen in Figure 26. The following figure show different moment curves and the shape parameters are listed below the figure.

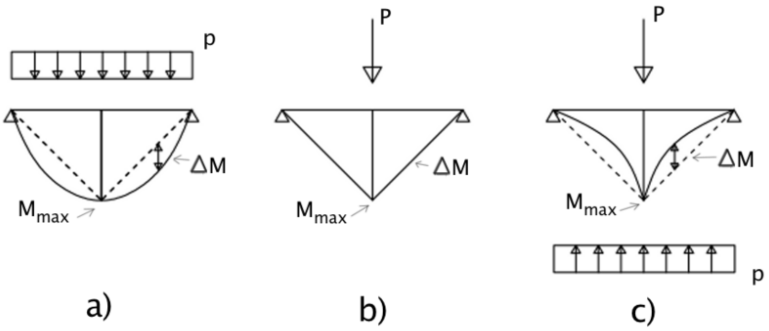

Figure 28: Defining shape parameter for: a) Sagging bending, b) Linear bending, c) Hogging bending

a) $\Delta M = -\frac{M_{max}}{4} \rightarrow \psi = -1$

b) $\Delta M = 0 \rightarrow \psi = 0$

c) $\Delta M = \frac{M_{max}}{4} \rightarrow \psi = 1$

If the flanges are stiffened in the longitudinal direction, see Figure 29, then β also depends on the cross sectional area of the stiffeners A_{sl} and the flange thickness t by a parameter κ.

$$\kappa = \alpha_0 \cdot b_0 \, / \, L_e \qquad 3.5$$

$$\alpha_0 = \sqrt{1 + \frac{A_{sl}}{b_0 \cdot t}} \qquad 3.6$$

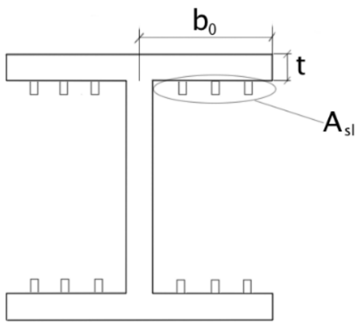

Figure 29: Flanges of I-section stiffened in longitudinal direction

L_e is defined as the distance between two adjacent points on the beam where the bending moment is zero, if no longitudinal stiffeners are used, κ only expresses the b_0 / L_e ratio. When Eq. 3.2 is solved and some simplifications are implemented, the following solution is provided, which only depend on the flange width b_0, the distance between points of zero bending moment L_e, and the shape parameter ψ.

$$\beta = \frac{1}{1 + 4(1+\psi)\frac{\alpha_0 b_0}{L_e} + 3{,}2(1-\psi)\left(\frac{\alpha_0 b_0}{L_e}\right)^2} \qquad 3.7$$

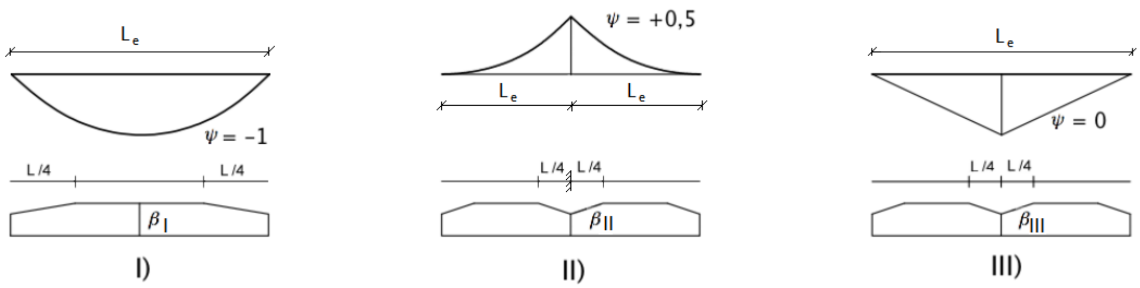

Figure 30: I) Effective width for sagging bending, II) effective width for hogging bending and III) the effective width calculated where linear bending is dominating [8]

Using Eq. 3.7 and the values for the shape parameter seen in Figure 30, the following equations for β_i are established.

I) Sagging bending:

$$\beta_I = \frac{1}{1 + 6{,}4 \cdot \kappa^2} \qquad 3.8$$

II) Hogging bending:

$$\beta_{II} = \frac{1}{1 + 6 \cdot \kappa + 1{,}6 \cdot \kappa^2} \qquad 3.9$$

III) Linear bending:

$$\beta_{III} = \frac{1}{1 + 4 \cdot \kappa + 3{,}2 \cdot \kappa^2} \qquad 3.10$$

3.1. Effective width according to EN 1993-1-5

In [2] a limit is set, above which the effect of shear lag does not have to be included.

$$L_e > 50 \cdot b_0 \tag{3.11}$$

Also a simplified way to determine the length L_e is provided. If no span is longer than 1½ times the adjacent span and a cantilever not longer than half the adjacent span then L_e may be determined from Figure 31. In all other situations L_e has to be determined by the distance between two adjacent points with zero bending moment [2].

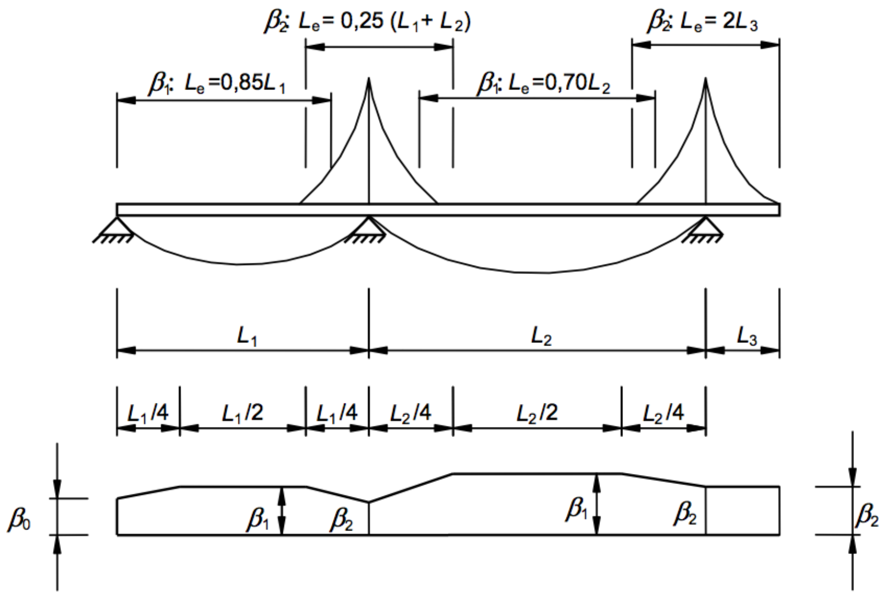

Figure 31: Definition of L_e for continuous simply supported beam and the associated β-values [2]

Formulas are given for β depending on the size of κ, and the shape of the bending moment curve, if it is sagging or hogging. A formula is also given for an end support and for a cantilever. For simplification the effective width is assumed to vary linearly from supports to sagging over one fourth of the beam length as seen in the lower part of Figure 31. Below is seen a table from [2] with the different formulas for β.

Table 2: Calculation of β depending on κ and shape of the bending moment curve shown in Figure 31 [2]

κ	location for verification	β – value
$\kappa \leq 0{,}02$		$\beta = 1{,}0$
$0{,}02 < \kappa \leq 0{,}70$	sagging bending	$\beta = \beta_1 = \dfrac{1}{1+6{,}4\,\kappa^2}$
	hogging bending	$\beta = \beta_2 = \dfrac{1}{1+6{,}0\left(\kappa - \dfrac{1}{2500\,\kappa}\right)+1{,}6\,\kappa^2}$
$> 0{,}70$	sagging bending	$\beta = \beta_1 = \dfrac{1}{5{,}9\,\kappa}$
	hogging bending	$\beta = \beta_2 = \dfrac{1}{8{,}6\,\kappa}$
all κ	end support	$\beta_0 = (0{,}55 + 0{,}025 / \kappa)\,\beta_1$, but $\beta_0 < \beta_1$
all κ	cantilever	$\beta = \beta_2$ at support and at the end
$\kappa = \alpha_0\, b_0 / L_e$ with $\alpha_0 = \sqrt{1+\dfrac{A_{s\ell}}{b_0 t}}$ in which $A_{s\ell}$ is the area of all longitudinal stiffeners within the width b_0.		

When the formula for hogging bending for $\kappa < 0.7$ from [2], is compared with Eq. 3.9 it is seen that an extra part is added in the denominator. The extra "$1/2500 \cdot \kappa$" added in [2] have influence for small κ values which is equivalent to long slender beams. For $\kappa = 0.02$ the β_2-value calculated according to [2] is 10.7 % higher than the β_{II} value according to Eq. 3.9, but the difference between the two β-values decreases rapidly for growing κ-values, and for $\kappa = 0.14$ the difference is less than 1%. The two β-values can be seen compared in Figure 32. No explanation has been found for the extra "$1/2500 \cdot \kappa$".

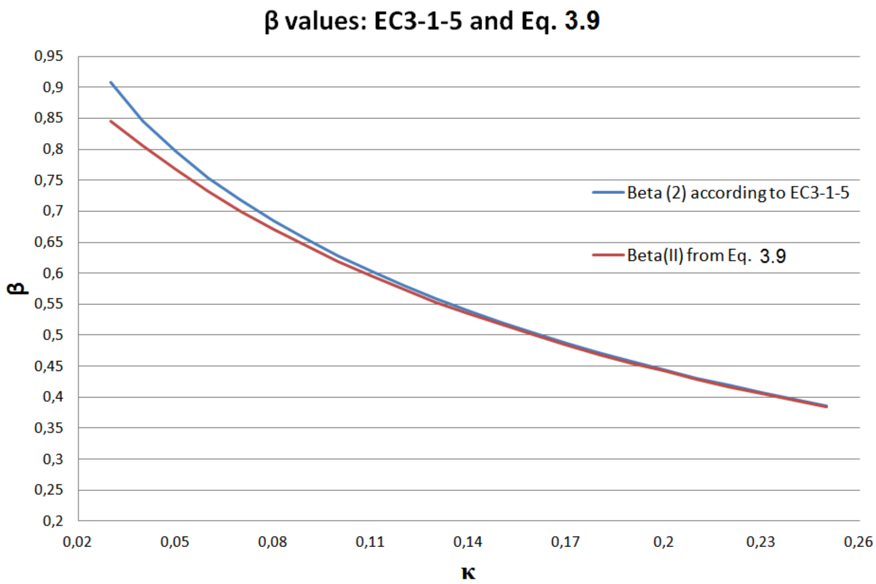

Figure 32: β-values described for hogging bending and κ < 0.7, according to EC3-1-5 and Eq. 3.9

β_1 in sagging bending for $\kappa < 0.7$ seen in Table 2 is similar to Eq. 3.8. The formulas for $\kappa > 0.7$ seen in Table 2 are relevant mostly for *stiffened* I-section beams. For beams without flange stiffening the span will be short compared to the width of the beam when $\kappa > 0.7$, and the stresses should be determined by an analysis of the end connections and not by using beam theory.

3.1.1. Example using formulas from EN 1993-1-5

A simply supported two span beam with a uniform load is used to express the effective width of an I-section beam relative to the length of the span. In Figure 33 the situation is seen. For simplicity no stiffeners of the flanges are included, and $\alpha_0 = 1$ in the following.

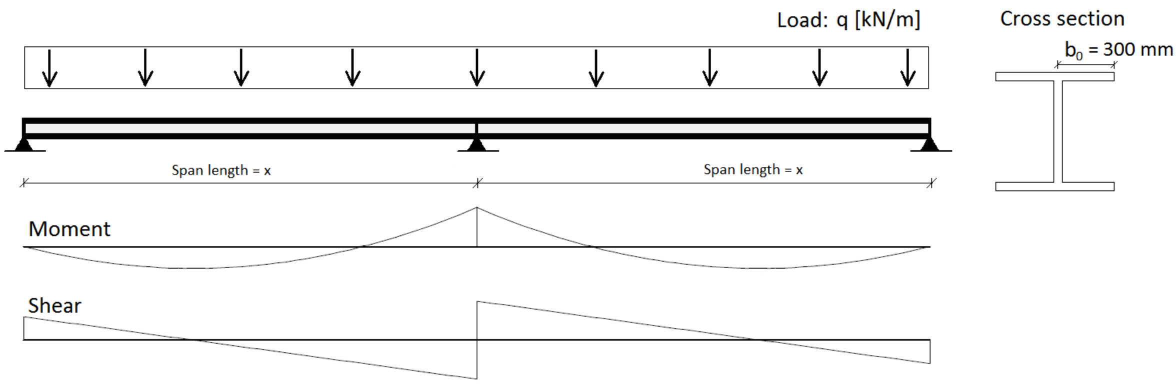

Figure 33: Simply supported two span beam with an uniform load and flange outstand b_0

Using the formulas from [2] for the effective width, see Table 2, and the situation seen in Figure 33, the effective width can be expressed for different span lengths.

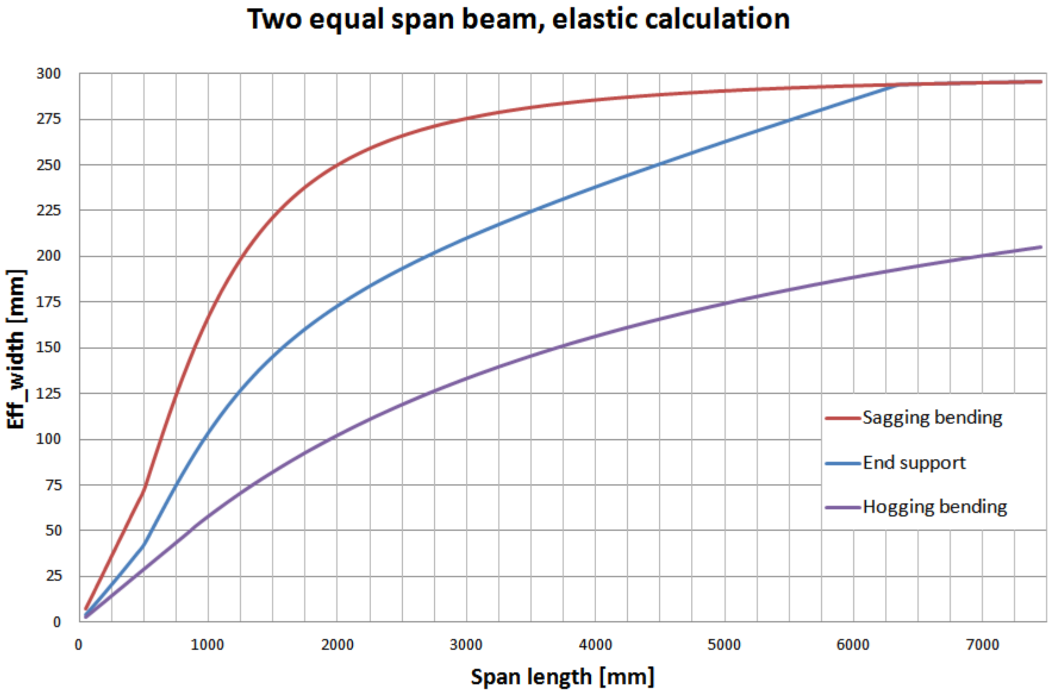

Figure 34: The effective width calculated by the formulas seen in Table 2 on a two equal span beam with b_0 = 300 mm and no stiffening of the flanges

The span length is the length between the supports, and the definition from Figure 31 has been used to calculate the length L_e, which describes the length between points where the bending moment is zero. With a full flange outstand of 300 mm the effective width can be seen for three situations from Figure 34. The red curve should be used where the bending moment curve describes sagging bending. Sagging bending gives the smallest reduction of the width. The blue curve describes the effective width at the beam-end if it is simply supported. The biggest reduction of the width is seen by the purple curve. This reduction should be used when the bending moment curve describes hogging bending, which is seen at the internal support on the two span beam in Figure 33.

4. Effective width from Ansys compared with equations from EN 1993-1-5

In section 3 it was described how EC3 calculates the effective width. In this section the width calculated by the formulas from [2] will be compared with the width calculated from a FE-Model. Ansys W. will be used to model a beam with 3 simple supports and a cantilever part, identical to the beam used to describe effective width in [2] see Figure 31. The modeled beam is a cross section class 1, and flange thickness and width is comparable with beams used on offshore structures. The web thickness also fits a real beam, but the web height is reduced to keep the cross section class to 1. The effective width in this section referrer to the flange outstand which is only half of the full flange width.

4.1. Composition of Ansys model

Design Modeler in Ansys W is used to model the beam. The geometry of the cross section can be seen in Figure 35.

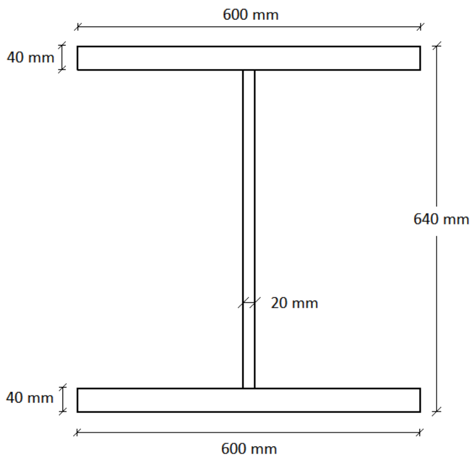

Figure 35: Cross section of modeled beam

The beam is simply supported to fit the conditions in Figure 31. In Ansys the support is applied by a displacement support = 0 in the direction of the load. All nodes in the height of the web are supported as seen in Figure 36.

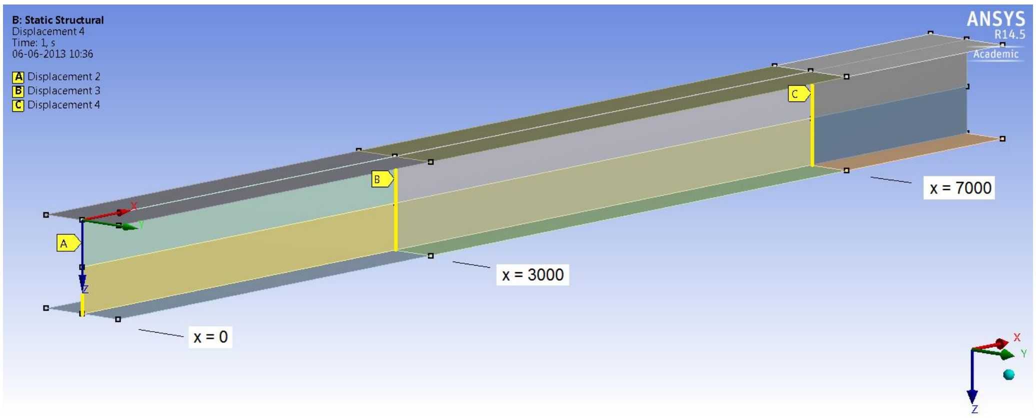

Figure 36: In the Ansys model all nodes in the web are displacement supported in the z-direction, at x = 0 mm, x = 3000 mm and at x = 7000 mm

The load is a line-pressure applied at the centre of mass of the beam. The situation is sketched in Figure 37 including the moment and shear curve. The first span in the model is 3 m and the second span is 4 m and the third span, which is a cantilever, is 1.5 m as seen in Figure 37.

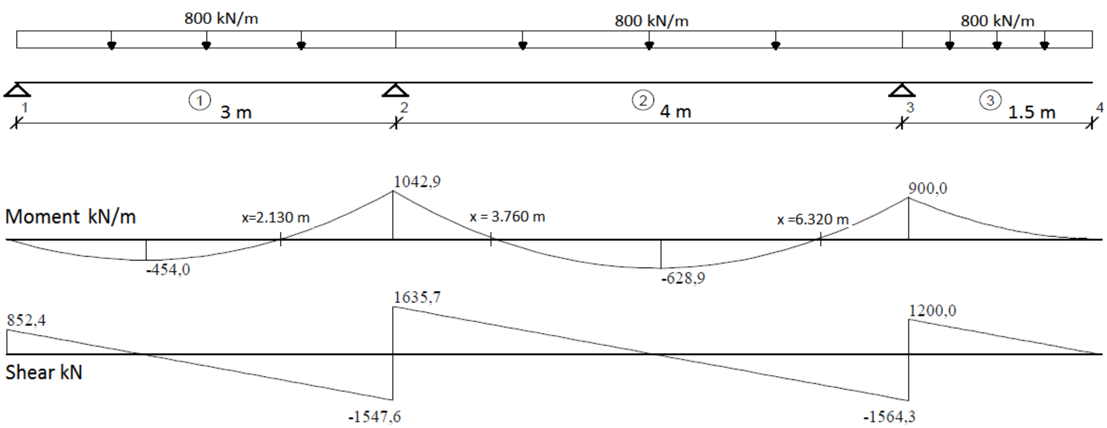

Figure 37: Load, moment and shear forces in the modeled beam

The model is meshed with SHELL281 elements with an increasing number of elements until the *structural error* converges as seen in Figure 38.

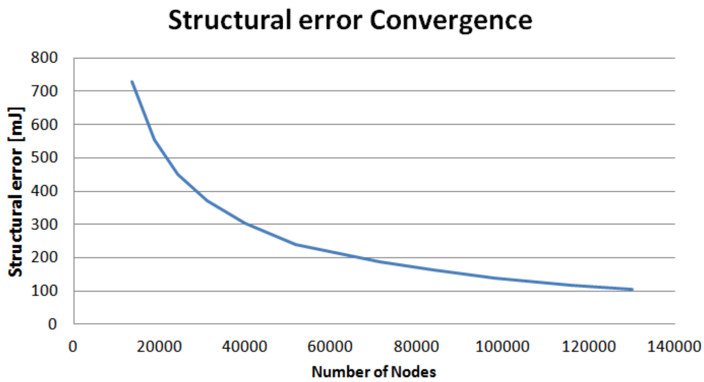

Figure 38: Convergence of structural error in the modeled three span I-beam

The flange is then meshed with 32 elements in the width as seen in Figure 39.

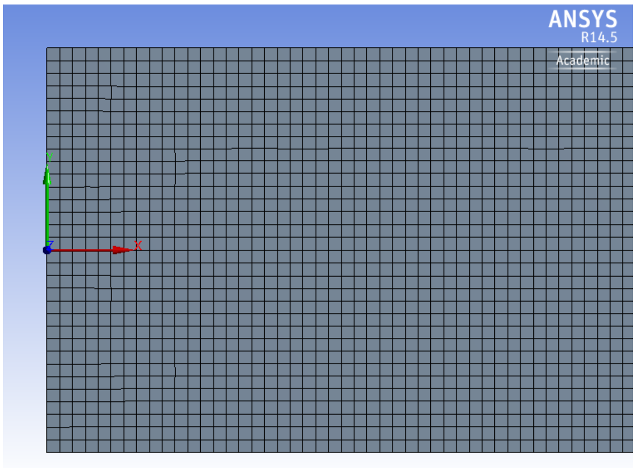

Figure 39: Refined mesh, top flange contains 32 elements in the width

The normal stress in the longitudinal direction of the beam can be seen in Figure 40. The stresses are seen both for the compression- and the tension-flange. As seen the size of the stresses are the same for the compression- as well as the tension-flange just with opposite sign. The tension flange will be used to calculate the effective width, even though both flanges could have been used in this example (linear model).

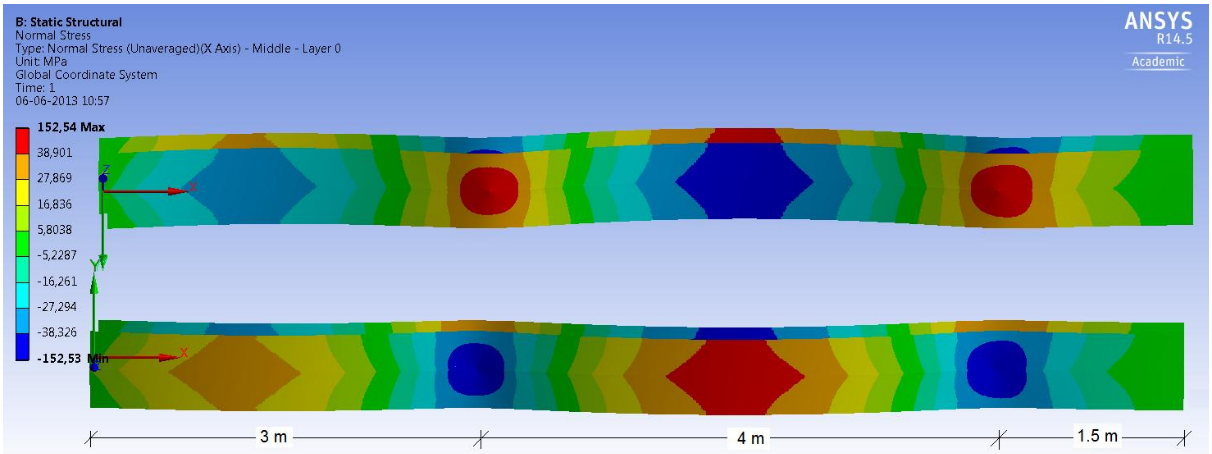

Figure 40: Normal stress in longitudinal direction of the modeled beam, compression flange is the upper and the tension flange is the lower

Element stresses are used to calculate the effective width as they express the mathematical purest stresses, (no averaging of stresses in the nodes).

4.1.1. Ansys effective width compared with equations from EN 1993-1-5

The effective width in the FE-Model is calculated from the tension flange by using Eq. 2.10 and 2.11. To be able to compare the results with effective widths calculated by the formulas from [2] in a diagram, the width calculated at the point of maximum moment is used for the middle half of the span. The effective width is assumed linear from supports to the width at maximum moment over one fourths of the span length. This is in accordance with the assumption in [2]. The effective width calculated at support 3 is used for the full length of the cantilever, also as described in [2].

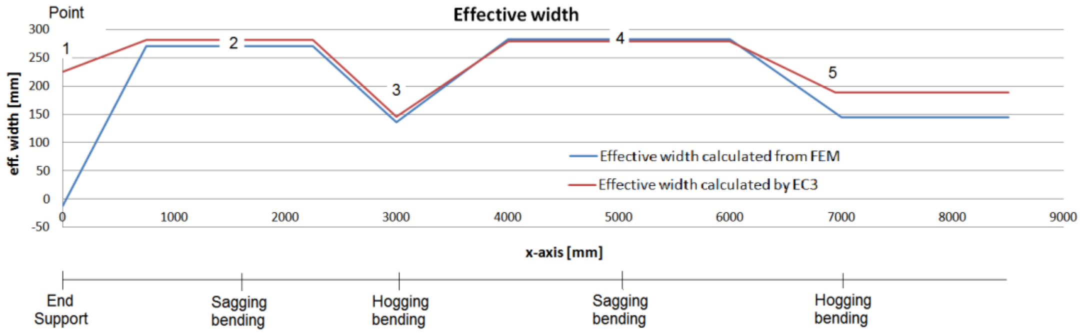

Figure 41: Effective widths calculated by formulas in [2] compared to effective widths calculated from a FE - Analysis in Ansys W. The width expresses one half of the total flange width

There is good agreement between the formulas from [2] and the FE-Analysis when the effective width is calculated for regions where the moment curve expresses sagging bending both in the first span and the second span. At support No. 2 (hogging bending) the two methods also has good agreement but the difference between the two methods are larger at the first support and at the last support. The effective width calculated from the FE-Analysis is smaller at all three supports where the moment curve expresses hogging bending. At the first span the FE calculated effective width is also smaller but in the second span the FE calculated width is a little bigger. The results are summed up in Table 3.

Table 3: Effective width calculated by the formulas from [2] and from the FE-Analysis using Eq. 2.10 and 2.11, the last row with *difference* show (EC3 – FEM)/FEM in %

Effective width	x = 0 [mm]	x = 750-2250 [mm]	x = 3000 [mm]	x = 4000-6000 [mm]	x = 7000-8500 [mm]
EN 1993-1-5	225.6	282.0	145.5	279.5	188.4
FEM	-11.9	270.3	128.2	282.6	144.4
Difference in %	-	4.3 %	13.5 %	-1.1%	38.2 %

At the first support the effective width calculated from the FE-Analysis is negative. To understand this, the normal stresses along a path from the web-flange joint to the flange edge are seen below.

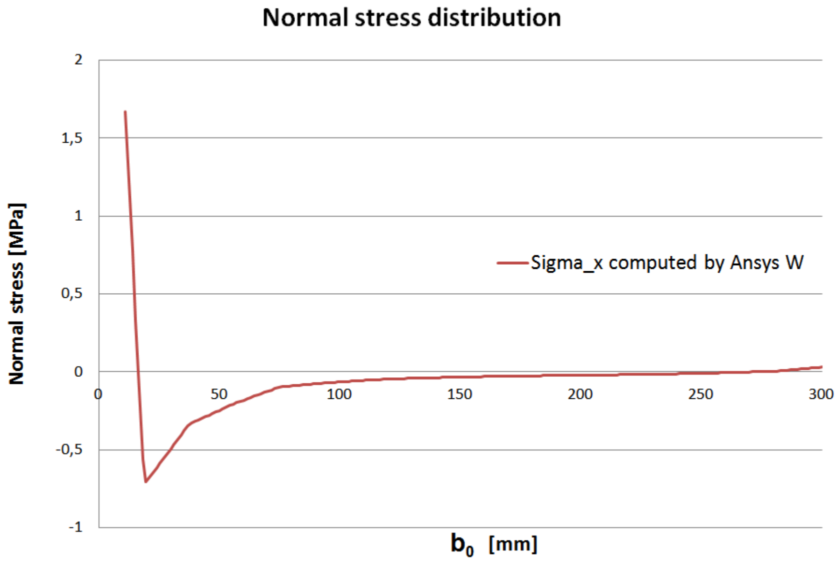

Figure 42: σ_x from the web / flange joint to the flange edge (y-coordinate 11 mm - 300 mm) at x = 0 mm

Right at the end support at x = 0 no stresses have developed away from the joint, and the flange is not yet activated here. Only the part of the flange closest to the web has been activated. Tension stresses are developed from the shear deformation close to the joint, but they soon reduce to almost nothing in the y-direction. When using Eq. 2.10 to calculate the effective width and both tension and compression stresses are present on the path evaluated, it is possible to get a negative effective flange width. It does not have a physical interpretation, and as it can be seen in Figure 42 the stresses are very low - below 2 MPa where they are highest.

At x = 100 mm the normal stresses have spread further in the y-direction as seen in Figure 43.

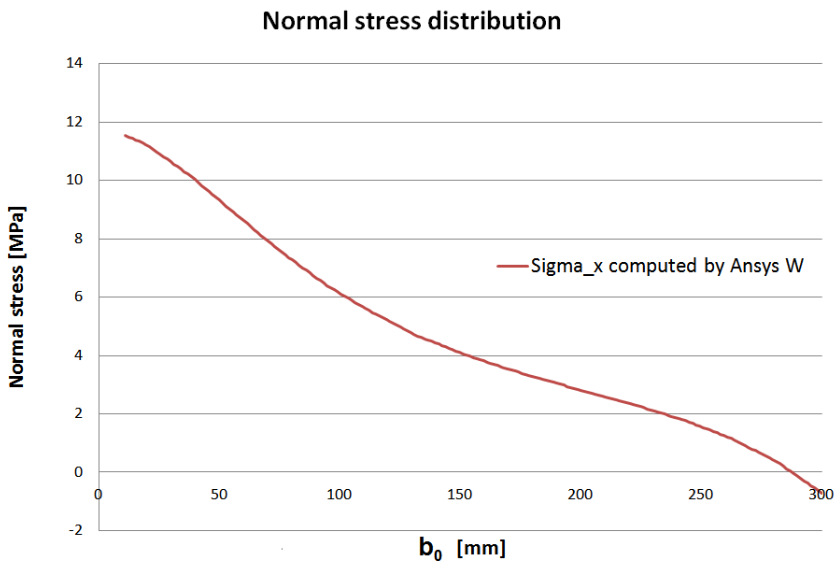

Figure 43: σ_x from the web-flange joint to the flange edge (y-coordinate 11 mm - 300 mm) at x = 100 mm

100 mm from the end support, the normal stresses are beginning to develop in the width of the flange but have still not activated the fibers at the edge of the flange, and therefore the effective width is still small. At x = 100 the moment in the beam is 8.5 kN/m and the shear force is 844.4 kN and the effective width is 122.1 mm. This width is 84.7 % smaller than the width calculated by the formulas from [2] at x = 0.

Referring to section 2.2 the small effective width at the end-support must be caused by the large shear stresses at the beam-end when the beam is simply supported.

At support No. 2 there is better agreement between to two compared methods, with a difference of 6.8 %.

At support No. 3 the effective width calculated from the FE-Analysis is 30.5 % smaller than the effective width calculated by the formulas from [2].

From the above it can be seen that when the stresses in the flange is caused only by the shear force leading to larger shear deformation in the web-flange joint, then the calculated effective width from the FE-Model is much smaller than when using the formulas from [2] seen e.g. at support No. 1. It is also seen that the shear force in general affects the effective width. When comparing the shear force distribution seen in Figure 37 with the calculated effective widths in Figure 41, it is seen that the width is smaller whenever the shear force is big. And where the moment is large and the shear force is zero, the calculated effective width is larger. The Ansys Workbench files used in this section can be found in App. (4).

5. Effective width from ROSAP compared with Ansys

As mentioned in the introduction beams on offshore topside structures are seldom simply supported in both ends, why the propagation of shear lag can be different from what is expected. In this section a part of a lifeboat support structure assessed by Ramboll Oil & Gas will be checked for shear lag both by ROSAP (Ramboll's in-house software), and from a model build up in Ansys W.

ROSAP is an abbreviation of: "Ramboll Offshore Structural Analysis Program Package". It's a software package developed by Ramboll and used for structural analyses. ROSAP is a finite element program consisting of several programs for static as well as dynamic analyses. A short presentation of the programs used from ROSAP in this report is following.

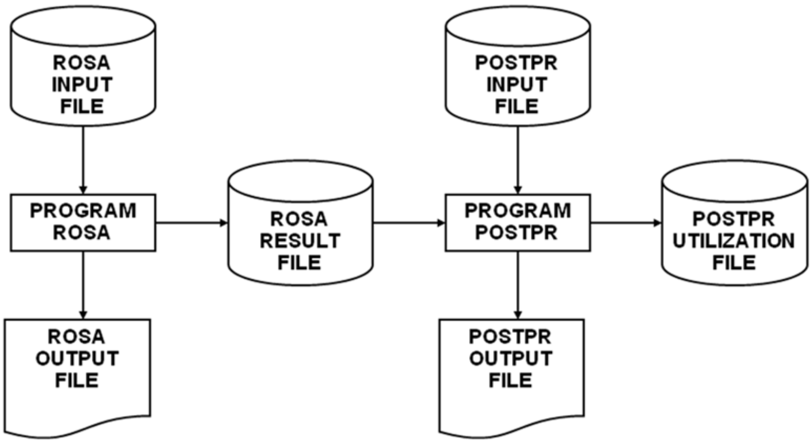

Figure 44: System diagram for program ROSA

Program ROSA "Ramboll Offshore Structural Analysis" is in this report used to analyze a later described structure. ROSA provides displacements of nodes and sectional forces for the structural elements, when provided with the structural geometry, load and stiffness properties.

Program STRECH "member stress analysis" is a post-processing program using an output file from ROSA to perform a stress check of the beam members in a given structure. STRECH is as default programmed to include shear lag in the stress calculation for all I- and Box-sections.

Program GLORIA "Interactive graphical display" is in this report used to perform plots of the structure with node names as well as loads. A system diagram for GLORIA is seen below.

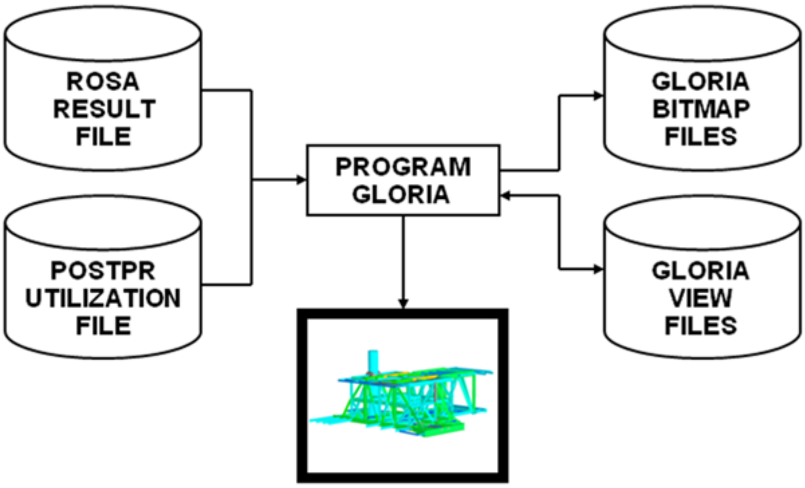

Figure 45: system diagram for program GLORIA

A lifeboat support structure is modeled and analyzed for shear lag both in ROSAP and in ANSYS, and the calculated flange width reduction factor β is compared between the two models.

As program STRECH is used to calculate shear lag in ROSAP, a more in depth introduction to this function in STRECH will follow in the next section, and also an explanation of some errors found in the way STRECH calculate shear lag is included in the following.

5.1. Program STRECH

This section gives a presentation of shear lag calculations in the post-processing program STRECH. Prior to a stress check in STRECH a static structural analysis in ROSA has been performed, as ROSA provides an output file used in STRECH for the stress check of the members in the analyzed structure. The stress check can be performed according to different specified codes but as shear lag is the focus, the check will be performed according to EC3 (DS/EN 1993-1-1:2007, [1], DS/EN 1993-1-5:2006, [2], [11], [12]).

In STRECH shear lag is calculated as default when EC3 is the chosen code for the check. It is allowed to neglect the effects of shear lag if the flange outstands are less than $L_e/50$ where L_e is the distance between points of zero bending moment, but this option is not used when shear lag is included in the stress check. Inclusion of shear lag is only possible for bending around the strong beam axis.

In general the un-braced lengths are taken as the node-to-node distance, unless compounds are introduced in program STRECH. A compound beam can be defined in STRECH if the individual beams are forming a straight line. Stresses are calculated in a number of defined stress points in each beam, and shear lag is determined for each stress point by calculating the length L_e for each stress point. A point of zero bending moment is defined every time the bending moment changes sign. See stress points and points of zero bending moment for a compound beam in Figure 46.

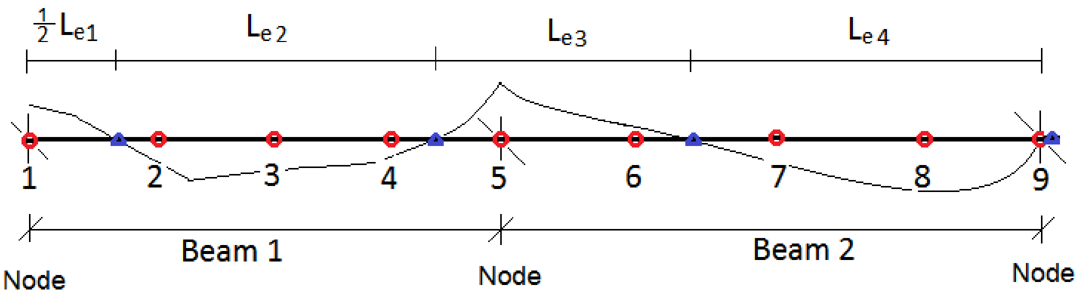

Figure 46: Bending moment curve, stress points marked with red and points with zero bending moment marked with blue, the two beams are assembled to a compound beam. As default 5 stress points are used in ROSA

When the two beams in Figure 46 are assembled to a compound beam, it influences the length L_{e3} at stress point 5 and 6. As compound beam L_e for point 5 and 6 is equal to L_{e3}. If they were not compounded the situation at point 1 would apply for point 5 in beam 1 and for point 5 and 6 in beam 2.

5.1.1. Errors detected in STRECH

In STRECH shear lag is calculated according to section 3.3 (Ultimate Limit State) in [2] and if a cross section class 4 is checked then local plate buckling is included. For cross sections in class 1, 2 and 3 local plate buckling is not included. According to the Danish National annex, NOTE 3 in section 3.3 in [2] should be chosen, which allow elastic-plastic shear lag effects by:

$$A_{eff} = A_{c,eff} \cdot \beta^{\kappa} \geq A_{c,eff} \cdot \beta \qquad 5.1$$

Where:

A_{eff}	is the effective cross section area
$A_{c,eff}$	is the effective[p] cross section area in the compression flange
β	is defined in Table 2
κ	is defined in Table 2

At each stress point the "flange width reduction factor" β is calculated according to [2] see Table 2. In STRECH β is calculated for *sagging* bending (β_1), *hogging* bending (β_2) and for *end-support* (β_0) at all stress points, and the minimum is chosen at each point.

$$\beta^{\kappa} = min(\beta_1^{\kappa}, \beta_2^{\kappa}, \beta_0^{\kappa}) \qquad 5.2$$

This approach can be illustrated by a two span beam with $L_1 = L_2$ and a uniform load.

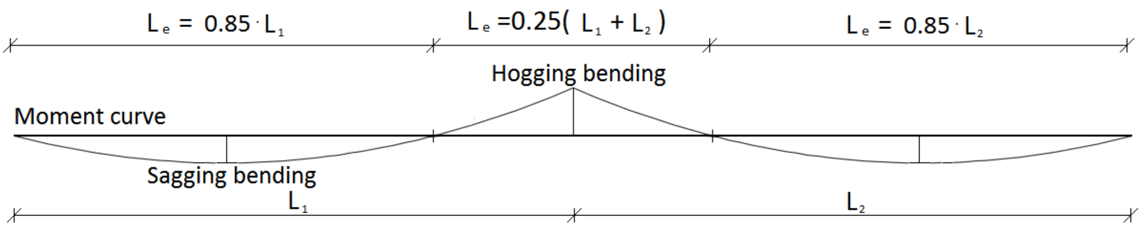

Figure 47: Moment curve for a two span beam, with definition of L_e for sagging bending and hogging bending according to [2]

The definition for L_e is from [2], and the β formulas for *sagging* bending, *hogging* bending and for the *end-support* can be seen in Table 2.

With a span length ($L_1 = L_2$) from 0 mm to 7500 mm the β-values are calculated in Microsoft Excel (for comparison) for the three situations (*sagging*, *hogging* and *end support*) and can be seen in Figure 48. The used profile is an I-section with flange outstands of 150 mm. The flange thickness and the profile height are not used in calculating the β-value when no flange stiffener is used.

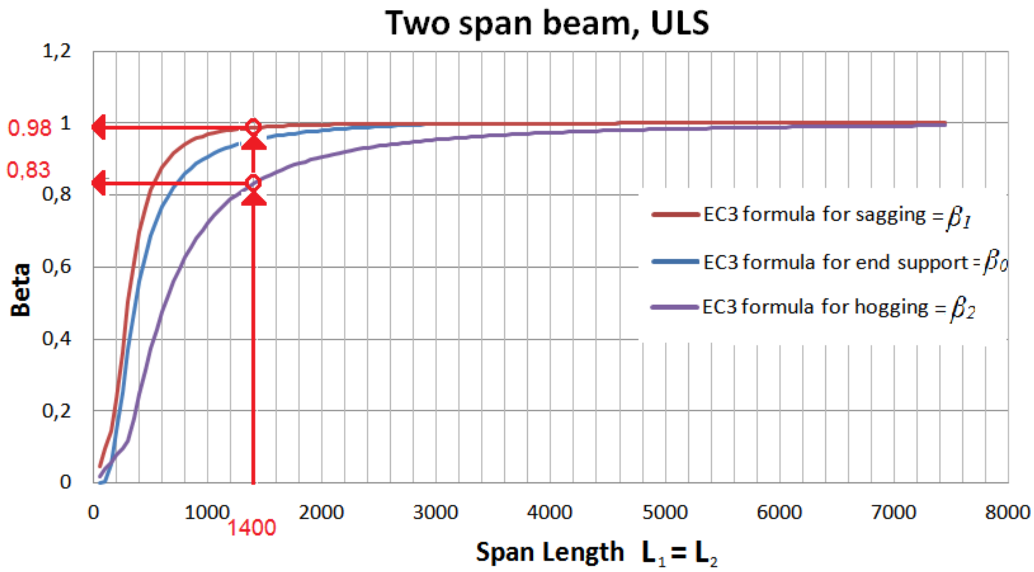

Figure 48: β_1, β_2, and β_0 calculated by the formulas from [2] for varying span length, the values are without inclusion of plasticity

For a span length of 1400 mm β_1 = 0.98 and β_2 = 0.83 (marked with red in Figure 48) giving a difference ($\beta_1 - \beta_2$) = 0.15 or a β_1 -value 18% larger than β_2. As β for *hogging* bending in this situation always is the minimum of the three, it will be the chosen value in STRECH, and must be seen as an error for a situation where the moment curve expresses *sagging* bending or at an *end support*.

In Figure 48 the curves for the β-values are made by using the definition for L_e from [2] (se Figure 31) and the formulas from [2] (see Table 2). A situation as seen in Figure 47 is modeled in ROSA and run with a number of varying span lengths. The output from ROSA is then run in the post-processor program STRECH, where the β-values are calculated and compared with the values from Figure 48. β-values are as default calculated in five stress points per beam. See an example of the calculated β-values from STRECH for a span length of 1.9 m in Table 4.

Table 4: Output from STRECH from a two span beam, here only the first span is seen, each span is 1.9 m, each beam is divided in 4 sub-elements giving 5 stress points where a β-value is calculated

E F F E C T I V E   P R O P E R T I E S ,   T A B L E   1

Dist ance (m)	Axial area (cm2)	Moments of inertia axis 1 (cm4)	axis 2 (cm4)	Eccentricity V-dir (mm)	W-dir (mm)	Angle (deg)	Sh.lag Le (m)	Plate buckl/shear lag red. factors upper left	upper right	lower left	lower right	web	Shear buck fact
0.00	108.1	6310	17512	0.0	0.0	0.00	1.48	1.000	1.000	1.000	1.000	1.000	1.000
								0.953	0.953	0.953	0.953		
0.47	108.1	6310	17512	0.0	0.0	0.00	1.48	1.000	1.000	1.000	1.000	1.000	1.000
								0.953	0.953	0.953	0.953		
0.95	108.1	6310	17512	0.0	0.0	0.00	1.48	1.000	1.000	1.000	1.000	1.000	1.000
								0.953	0.953	0.953	0.953		
1.42	108.1	6310	17512	0.0	0.0	0.00	1.48	1.000	1.000	1.000	1.000	1.000	1.000
								0.953	0.953	0.953	0.953		
1.90	101.6	6310	16282	0.0	0.0	0.00	0.84	1.000	1.000	1.000	1.000	1.000	1.000
								0.876	0.876	0.876	0.876		

The modeled beam is a cross section class one and hence no reduction is done for local plate buckling, it can be seen as the reduction factor for plate buckling is 1.000 in Table 4 (seen above the marked β-values). The flange outstand is 150 mm as used in the Excel example, and as the load is equal distributed over the whole beam and only in the plane of the beam, the β-value is the same for all four flange outstands (upper left, upper right, lower left, lower right).

In the first stress point the β-value from STRECH is *0.953* which is equal to the value at distance 0.47 m, 0.95 m and at 1.42 m (stress point 2, 3 and 4). In STRECH β-values are calculated for *sagging*, *hogging* and *end support*; at each stress point, and the smallest value is chosen as seen in the following. The length L_e used in the calculation can be seen for each β in Table 4 and STRECH uses elastic-plastic β-values see Eq. 5.1.

β_1^{κ} (*sagging*) in the first stress point ($\kappa = b_0/L_e$ = 150 mm / 1480 mm = 0.10):

$$\beta_1^{\kappa} = \left(\frac{1}{1 + 6.4 \cdot 0.10^2}\right)^{0.10} = 0.994 \qquad 5.3$$

β_2^{κ} (*hogging*) in the first stress point ($\kappa = b_0/L_e$ = 150 mm / 1480 mm = 0.10):

$$\beta_2^{\kappa} = \left(\frac{1}{1 + 6.0\left(0.10 - \frac{1}{2500 \cdot 0.10}\right) + 1.6 \cdot 0.10^2}\right)^{0.10} = 0.953 \qquad 5.4$$

β_0^{κ} (*end support*) in the first stress point ($\kappa = b_0/L_e$ = 150 mm / 1480 mm = 0.10):

$$\beta_0^{\kappa} = \left((0.55 + 0.025/0.10)\beta_1\right)^{0.10} = 0.971 \qquad 5.5$$

In STRECH the chosen β-value (the minimum calculated for the first stress point) is for *hogging*; $\beta_2^{\kappa} = 0.953$ which is not correct as the first stress point is an *end support*, and the β-value should be: *0.971*. The next three stress points uses the same L_e as the first stress point, and again STRECH chooses the *hogging* β_2^{κ}-value, but here the right value should be $\beta_1^{\kappa} = 0.994$ for *sagging* bending. In the last stress point for the first span the L_e length is 0.84 m giving a $\kappa = 0.18$. Here the bending moment curve expresses *hogging* bending and STRECH chooses the right β-value.

$$\beta_2^{\kappa} = \left(\frac{1}{1 + 6.0\left(0.18 - \frac{1}{2500 \cdot 0.18}\right) + 1.6 \cdot 0.18^2}\right)^{0.18} = 0.876 \qquad 5.6$$

The error caused by using the minimum β-value in all stress points is seen for each point in Table 5.

Table 5: By always using the minimum β-value, STRECH overestimates the shear lag effect

	Point 1	Point 2	Point 3	Point 4	Point 5
EC3	0.971	0.994	0.994	0.994	0.876
STRECH	0.953	0.953	0.953	0.953	0.876
Error STRECH vs EC3	+1.9 %	+4.1 %	+4.1 %	+4.1 %	0 %

When comparing the β-values in *hogging* from STRECH for a number of span lengths with those calculated by the formula for *hogging* bending, they would be expected to be equal, which also is the case as seen in Figure 49.

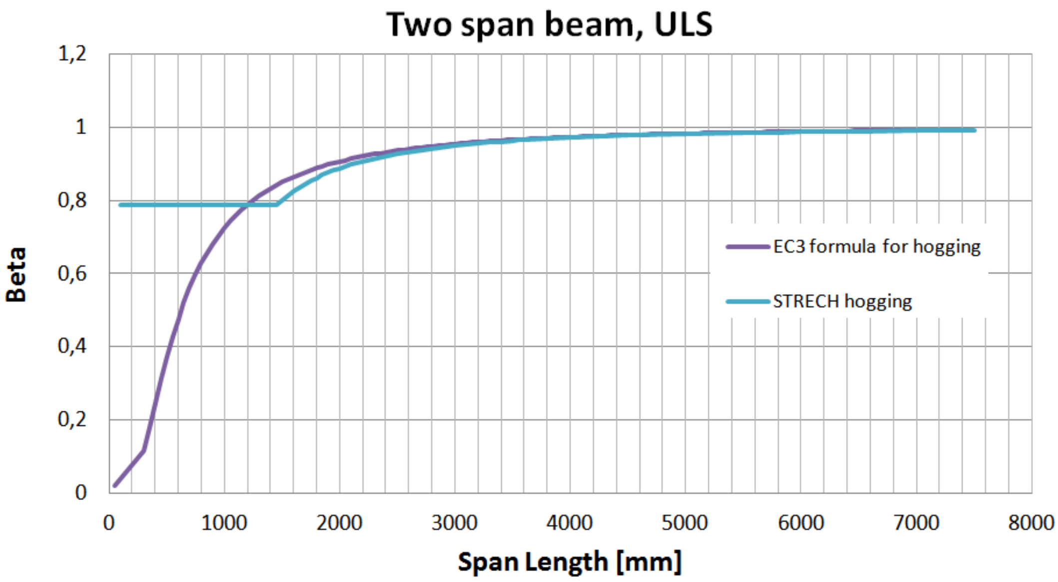

Figure 49: β values calculated by the formula for hogging from [2] and by STRECH in the last point of the first span. A large number of span lengths have been run to make the curve see App. (5)

In STRECH a minimum L_e has been set to twice the flange width, to avoid calculating shear lag in very short beams where beam theory doesn't give the correct answer. As seen in Figure 49 this limit is reached at a beam length of 1.5 m. Above 1.5 m STRECH calculates a β-value a little lower than the one calculated in Excel by the formula for *hogging* from [2] which must be explained by L_e calculated as $0.25(L_1 + L_2)$ for the EC3 curve and by the moment-distribution for the STRECH curve.

In STRECH the β-values in the first four stress points are the same and as shown STRECH uses the "hogging value" based on the calculated L_e. In Figure 50 this value is compared with the values, which should have been chosen for *end support* and *sagging* bending respectively.

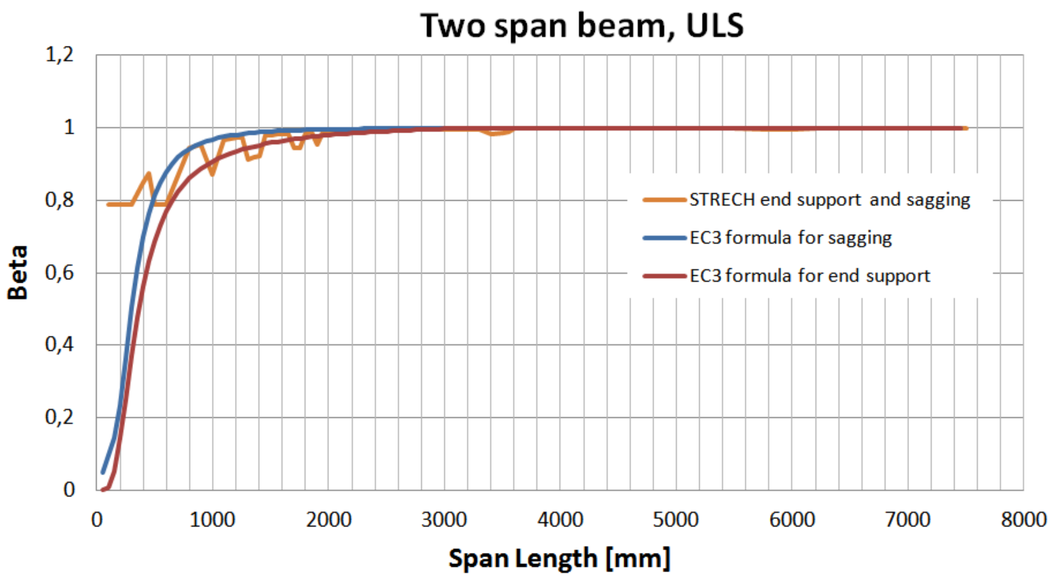

Figure 50: β values calculated by the formula for sagging and for end support in Excel and by STRECH in the first four stress points.

In the first four stress points in the first span of the two span beam, STRECH calculates the same β-value, see Table 4, and as seen in Figure 50 something is not right. As STRECH uses the same formulas as EC3 to calculate the β-values the only variable that can cause the curve to jump as seen in Figure 50 is the length L_e. In STRECH L_e is calculated as the distance between points of zero bending moment and points of zero bending moment is defined between two stress points with different sign for the bending moment. Examples from the output from STRECH are seen below with span lengths of 1850 mm and 1900 mm respectively.

Table 6: The L_e length for a span of 1.85 m in five stress points

E F F E C T I V E   P R O P E R T I E S ,   T A B L E   1

Distance (m)	Axial area (cm2)	Moments of inertia axis 1 (cm4)	Moments of inertia axis 2 (cm4)	Eccentricity V-dir (mm)	Eccentricity W-dir (mm)	Angle (deg)	Sh.lag Le (m)	Plate buckl/shear lag red. factors upper left	upper right	lower left	lower right	web	Shear buck fact
0.00	111.0	6310	18062	0.0	0.0	0.00	2.88	1.000	1.000	1.000	1.000	1.000	1.000
								0.988	0.988	0.988	0.988		
0.46	111.0	6310	18062	0.0	0.0	0.00	2.88	1.000	1.000	1.000	1.000	1.000	1.000
								0.988	0.988	0.988	0.988		
0.93	111.0	6310	18062	0.0	0.0	0.00	2.88	1.000	1.000	1.000	1.000	1.000	1.000
								0.988	0.988	0.988	0.988		
1.39	111.0	6310	18062	0.0	0.0	0.00	2.88	1.000	1.000	1.000	1.000	1.000	1.000
								0.988	0.988	0.988	0.988		
1.85	101.0	6310	16173	0.0	0.0	0.00	0.82	1.000	1.000	1.000	1.000	1.000	1.000
								0.870	0.870	0.870	0.870		

Table 7: The L_e length for a span of 1.9 m in five stress points

E F F E C T I V E   P R O P E R T I E S ,   T A B L E   1

Distance (m)	Axial area (cm2)	Moments of inertia axis 1 (cm4)	Moments of inertia axis 2 (cm4)	Eccentricity V-dir (mm)	Eccentricity W-dir (mm)	Angle (deg)	Sh.lag Le (m)	Plate buckl/shear lag red. factors upper left	upper right	lower left	lower right	web	Shear buck fact
0.00	108.1	6310	17512	0.0	0.0	0.00	1.48	1.000	1.000	1.000	1.000	1.000	1.000
								0.953	0.953	0.953	0.953		
0.47	108.1	6310	17512	0.0	0.0	0.00	1.48	1.000	1.000	1.000	1.000	1.000	1.000
								0.953	0.953	0.953	0.953		
0.95	108.1	6310	17512	0.0	0.0	0.00	1.48	1.000	1.000	1.000	1.000	1.000	1.000
								0.953	0.953	0.953	0.953		
1.42	108.1	6310	17512	0.0	0.0	0.00	1.48	1.000	1.000	1.000	1.000	1.000	1.000
								0.953	0.953	0.953	0.953		
1.90	101.6	6310	16282	0.0	0.0	0.00	0.84	1.000	1.000	1.000	1.000	1.000	1.000
								0.876	0.876	0.876	0.876		

As seen in Table 6 and Table 7 the L_e length varies a lot when the span length only varies 50 mm and this has to be explained by how STRECH defines points of zero bending moment. If the bending moment between two stress points switches from a positive moment to a negative moment, then STRECH define a point with zero bending moment between these two points.

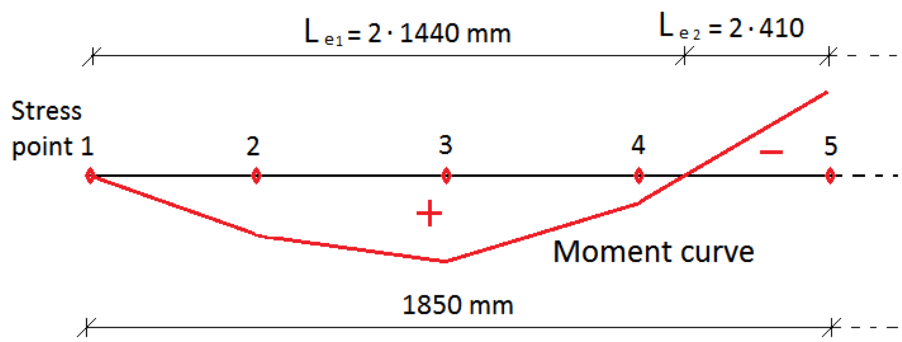

Figure 51: Moment curve and calculation of L_e in STRECH

Knowing that the bending moment in stress point 1 should be zero, but if a numerical very small positive moment is calculated in STRECH then only one point of zero bending moment is defined in the span, and L_e is calculated as twice the distance from the point of zero bending moment and the end of the beam.

If a very small negative moment is calculated by STRECH in point 1, then two points of zero bending moment is registered in the span, and L_e is equal to the distance between these two points for the first four stress points.

In the example with a span length of 1850 mm L_e should have been 1440 mm for the first part of the span, but STRECH uses a L_e two times 1440 and this causes the error seen in Figure 50 on the graph with β-values calculated by STRECH.

In the example with a span length of 1900 mm STRECH calculates a L_e of 1480 mm for the first part of the span. This gives a much smaller value for β and as it looks coincidental if STRECH uses the right L_e or twice the right L_e.

Over the internal support where the bending moment curve expresses *hogging* bending, STRECH calculates the right L_e which is the distance between the two closest points of zero bending moment in the two spans, or twice the distance from the point of zero bending moment and the internal support. In this situation it is the same as the two span lengths are the same and equally loaded. It should be mentioned that the two beams forming the two spans not have been calculated as a compound beam in ROSA, but that should not bring any change to the result in the used example.

In Table 8 the error caused by calculating the wrong L_e for the first four stress points is seen, the span length is 1.85m. The error does not include the error from Table 5 caused by using the wrong β-value in the first four points of the first span.

Table 8: Error caused by using twice the L_e for a span length of 1.85 m

	Point 1	Point 2	Point 3	Point 4	Point 5
STRECH with $2 \cdot L_e$	0.988	0.988	0.988	0.988	0.876
STRECH With 1 • Le	0.951	0.951	0.951	0.951	0.876
Error	3.9 %	3.9 %	3.9 %	3.9 %	0 %

As STRECH in the first described error overestimates the reduction factor, and in this second error underestimates the reduction factor when a wrong L_e is used, they equalize each other when both are present in a calculation.

All the ROSAP data from the performed tests in this section can be found in App. (5).

5.2. Shear lag check made by ROSAP

As mentioned in the introduction to section 5 a lifeboat support structure has been analyzed for shear lag by the ROSAP software. Focus is on one compound beam in this structure, as the engineers had problems with the effect of shear lag in this beam when the structure was assessed. Check of the original design was done by using the ROSAP software. In the following this structure is described with dimensions, supports and loads. The maximum directional displacement will be calculated by ROSA, and later compared with the displacement calculated in a copy of the structure modeled with shell elements in Ansys. This is done to verify that the Ansys shell model is acceptable. Finally *β*-values will be compared between the two FEM programs.

5.2.1. Analyzed structure in ROSA

The structure is a part of a lifeboat support and placed on an offshore platform in the North Sea. A drawing of the main deck structure is seen below. The analyzed beam is marked with red. More detailed drawings of the structure are found in App. (6).

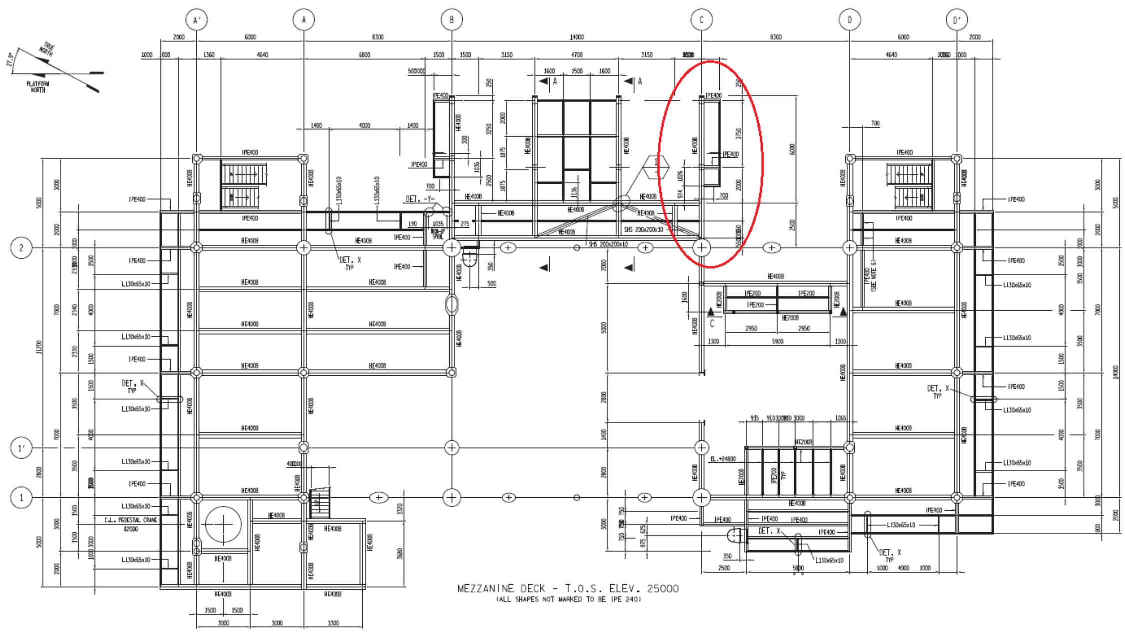

Figure 52: Main structure of the deck where the lifeboat support is placed

Some simplifications of the structure have been made. One beam is analyzed for shear lag, and the structure is simplified to 2D, and all loads are in the plane of the looked at structure. The analyzed structure can be seen in Figure 53.

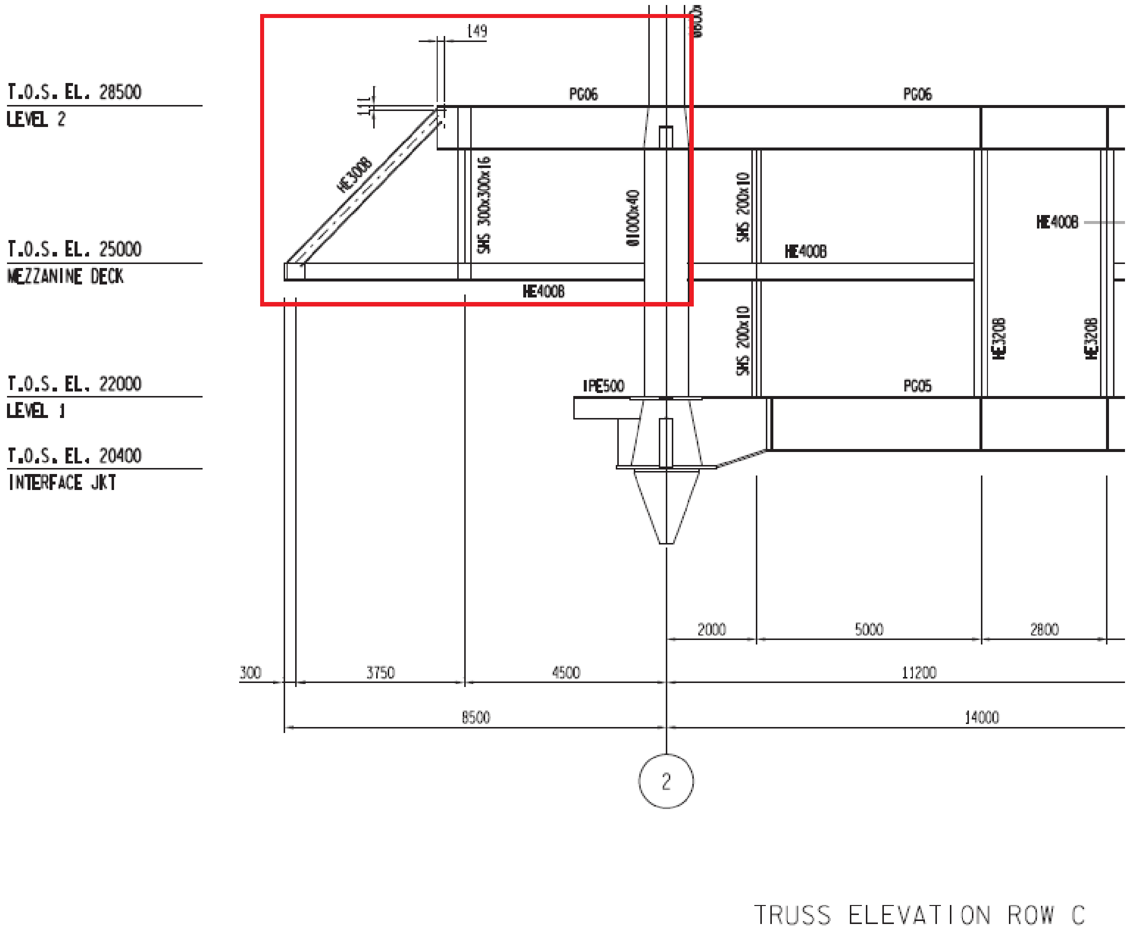

Figure 53: Lifeboat support structure where the lower horizontal beam HE400B is checked for shear lag

The structure seen in the red box in Figure 53 is modeled in ROSA and later in Ansys W. and the flange width reduction factor β will be compared between the two models. Another change has been made to the model; the vertical beam has been changed from a pipe section to an I-section. It was found that copying the structure to a shell model in Ansys was much easier with an I-section beam than with a pipe section, and as it was done in both models it was assessed to be ok. A plot of the modeled structure in ROSA made by program GLORIA is seen below, where loads, boundary conditions and beam numbers have been added.

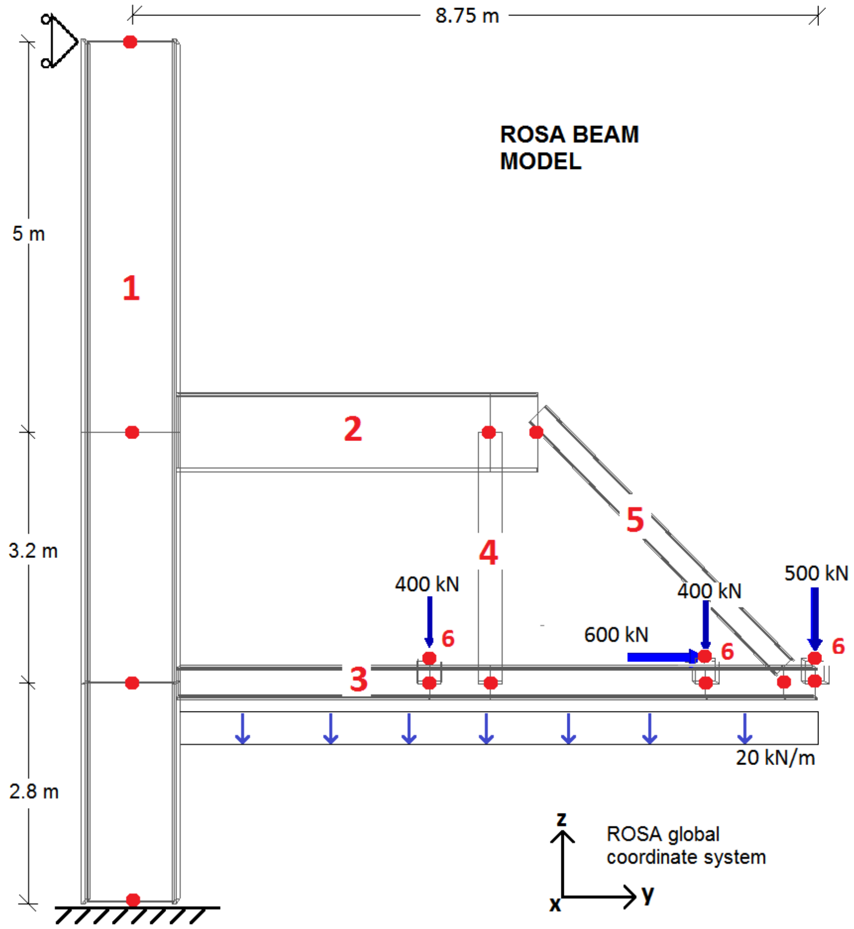

Figure 54: Load, boundary conditions and beam numbers for lifeboat structure, modeled in ROSA and plotted by program GLORIA

In Figure 54 all the different sections have been numbered and the dimensions are described in Table 9. The point loads are applied on SHS300 sections (numbered with 6 in Figure 54) at a distance of 290 mm from the center of *beam 3*. This will give a moment in beam 3 where the horizontal point load is applied. The equal distributed load on *beam 3* is applied in the full length of *beam 3*. Also a gravity load of 9.807 m/s^2 is applied in the negative z-direction to the full structure.

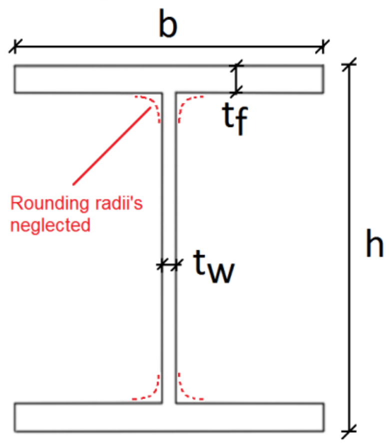

Figure 55: Double symmetric I-section

Table 9: Dimensions for double symmetric I-sections and SHS sections in the structure

Beam No.	**Cross section**	**h** [mm]	t_w [mm]	**b** [mm]	t_f [mm]
1	I-section	1200	42	300	45
2	I-section	1000	20	300	40
3	I-section	400	13.5	300	24
4	SHS-section	300	16	300	16
5	I-section	300	11	300	19
6	SHS-section	300	16	300	16

The material properties used in the structure are listed in Table 10.

Table 10: Material properties in the structure

Upper limit of thickness [mm]	Modulus of elasticity: E [MPa]	Shear modulus: G [MPa]	Poisson's ratio: ν	Mass density [kg/m^3]	Yield strength [MPa]
16.0	205000	78846.2	0.3	7850.0	355
40.0	205000	78846.2	0.3	7850.0	345
63.0	205000	78846.2	0.3	7850.0	335

Beam 2 and *3* are given an offset of 600 mm in the positive y-direction for their left node. This is done for the beams to deform correctly in the z-direction when the load is applied. See Figure 56.

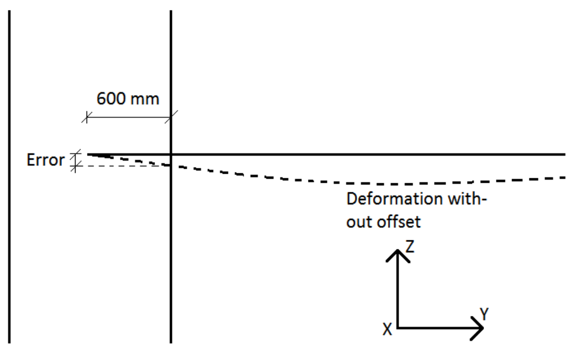

Figure 56: Deformational error if the offset is not applied

Beam 5 is given an offset of 236 mm in the upper node and 200 mm in the lower node, both in the positive z-direction. This is done for the model to fit the physical structure.

No releases are applied in the model, so all connections between elements are stiff.

The boundary conditions are as follow: *Beam 1* is fixed at the bottom node in all 6 degrees of freedom. At the top node *beam 1* is fixed for translation in the x- and y-direction and free in z-direction and all rotational degrees of freedom are free as well also sketched in Figure 54.

The displacements calculated by ROSA are seen in Table 11, where the right end node of *beam 3* is circled with red having a value of 47.98 mm. This displacement will later be compared with the displacements calculated in the Ansys shell model.

Table 11: Node displacements, right end node of *beam 3* is circled in red

Program ROSA PROJECT : 2013-05-16 Page
Version 4.70 SUBJECT : 10.08 Hrs 15

N O D E D I S P L A C E M E N T S

Node name	Comb load case	Translations direc. X (mm)	Translations direc. Y (mm)	Translations direc. Z (mm)	Rotations direc. X (rad)	Rotations direc. Y (rad)	Rotations direc. Z (rad)
A0P010	1	0.00	0.00	0.00	0.00000	0.00000	0.00000
A0P020	1	0.00	1.19	-0.29	-0.00128	0.00000	0.00000
A0P220	1	0.00	0.73	-25.65	-0.00705	0.00000	0.00000
A0P520	1	0.00	0.62	-30.15	-0.00510	0.00000	0.00000
A0P720	1	0.00	0.40	-44.79	-0.00376	0.00000	0.00000
A0P820	1	0.00	0.17	-46.56	-0.00198	0.00000	0.00000
A0P920	1	0.00	0.17	-47.98	-0.00233	0.00000	0.00000
A0P221	1	0.00	2.78	-25.68	-0.00705	0.00000	0.00000
A0P721	1	0.00	1.86	-44.83	-0.00427	0.00000	0.00000
A0P921	1	0.00	0.85	-48.01	-0.00233	0.00000	0.00000
A0P030	1	0.00	6.62	-0.53	-0.00190	0.00000	0.00000
A0P530	1	0.00	7.15	-29.93	-0.00847	0.00000	0.00000
A0P630	1	0.00	7.22	-35.43	-0.00858	0.00000	0.00000
A0P040	1	0.00	0.00	-0.54	0.00247	0.00000	0.00000

Names of all the nodes can be seen in Figure 57.

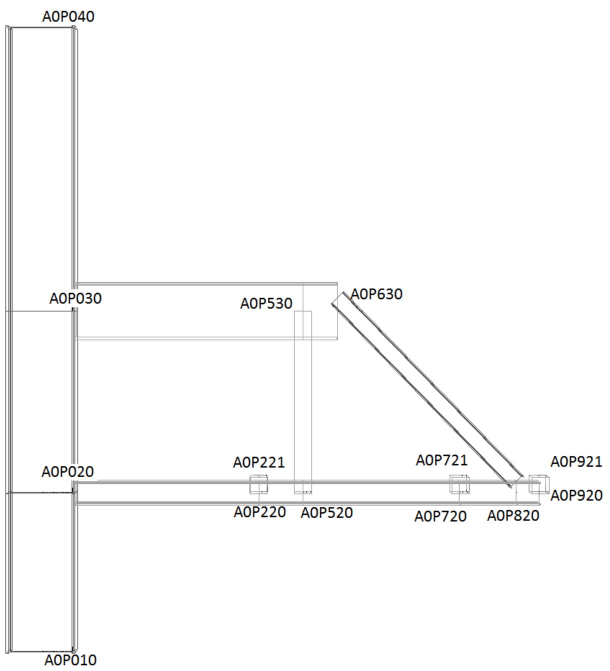

Figure 57: Node names of all nodes in the structure

5.2.2. β-values computed by STRECH

Beam 3 in the structure is checked for shear lag effects. The beam consists of 5 individual beams assembled to one compound beam. Each of the five beams has 5 stress points, and stress points between beams are shared points. If the shared point is a point of zero bending moment, two β-values for the point is calculated, one for each beam *part*. An example is seen from the actual bending moment curve for the compound *beam 3* in Figure 58 for the described load case.

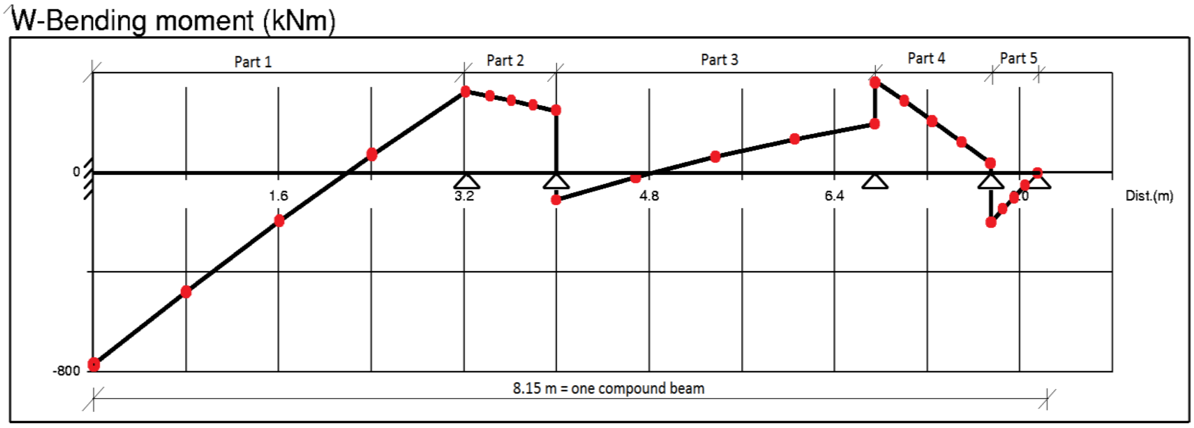

Figure 58: Bending moment curve for *beam 3*, stress points are marked with red

In the shared point between part 2 and part 3, two different L_e lengths are calculated. When β is calculated for the last point in part 2, L_e is found by looking for the nearest point of zero moment to the left, and when β is calculated for the first point in part 3, L_e is found by looking for the nearest point of zero moment to the right. This gives two different β-values for the same point, and when this is the case, the smallest β-value is chosen in the following. The error with sometimes choosing the wrong L_e in STRECH described in section 5.1.1 has not happened in this analysis. The distance between the last two points of zero bending is 400 mm. STRECH uses a distance of 800 mm, and as the moment curve could be characterized as *hogging* bending, choosing L_e as twice the actual length is assessed to be acceptable. But the other described error of always choosing the minimum β-value (*hogging* value) in each point is done in STRECH and it can be discussed if this actually is the form of the bending moment curve, or a formula for a linear bending moment curve should have been used.

The β-values calculated by STRECH in *beam 3* can be seen in Figure 59.

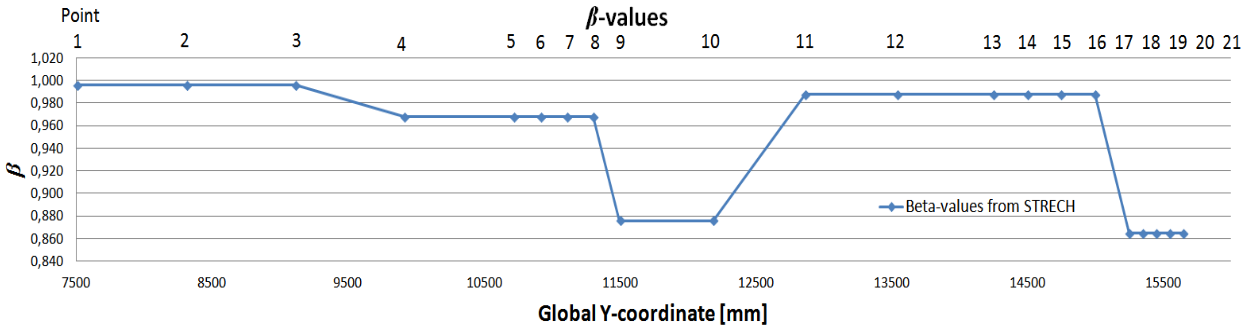

Figure 59: β-values calculated by STRECH for *beam 3*, x-axis on the figure is the global beam axis (y-axix)

As seen in Figure 59; STRECH calculate rather large reduction factors at two places along the beam. The input and output data from the ROSAP analysis can be seen in App. (6) together with detail drawings of the modeled structure. In the next section the same structure is modeled in Ansys, and reduction factors are calculated and compared with those from STRECH.

5.3.Shell model in Ansys Workbench

The structure described in section 5.2.1 is also modeled in Ansys W. using Design Modeler. As seen earlier Ansys provides a good description of how the stresses propagate in a beam modeled with shell elements, and with a good model it is expected to be the most precise way to calculate the flange reduction factor β. The β-values will be calculated from the Ansys model for *beam 3*, and in section 5.4 they will be used as a reference for the β-values calculated by STRECH seen in Figure 59. In this section the construction of the model in Ansys Design Modeler and in Ansys Mechanical will be explained.

A coordinate file with all necessary points have been made and imported to Design Modeler, and the "Lines From Points" function has been used to construct the structure from the points as seen in Figure 60.

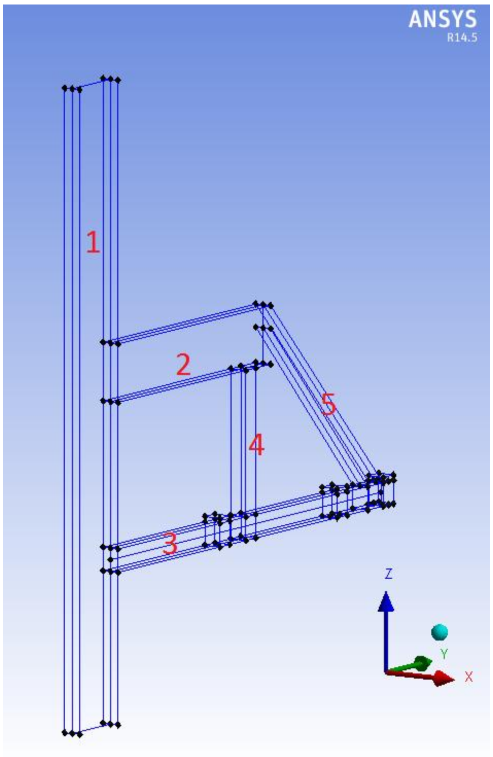

Figure 60: A coordinate file is loaded into Design Modeler, and the necessary lines drawn

From the lines the faces are defined in Design Modeler without thickness. In Ansys Mechanical the thickness for all faces are added to give the individual beams the right dimensions. The used material properties and dimensions can be seen in Table 9 and Table 10.

The connection between the vertical *beam 1* and the two horizontal *beams 2* and *3* is performed with web stiffeners as seen in Figure 61. In the ROSA model these connections are stiff and to ensure that the forces and moments in the Ansys model are transferred correctly the web stiffeners are implemented. Web stiffeners are also implemented in *beam 3* in the connections with *beam 4* and *5*.

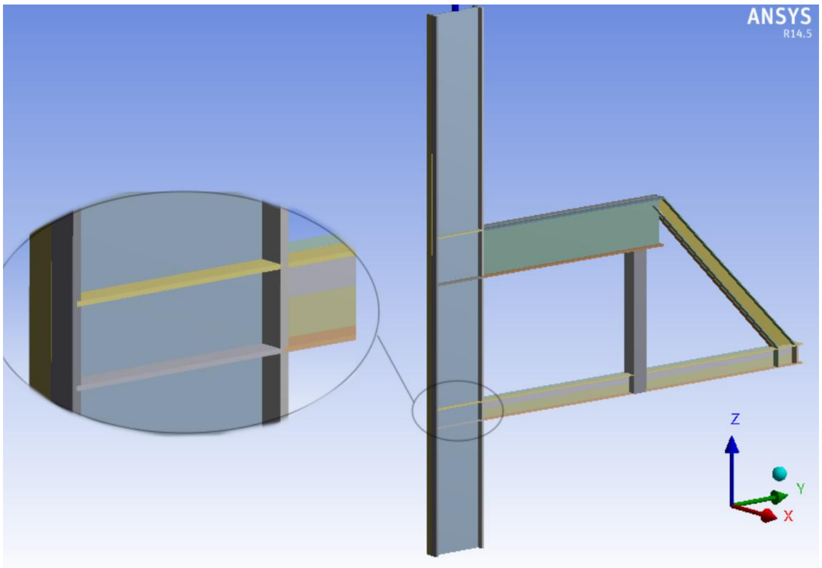

Figure 61: Web stiffener on the vertical beam

The Ansys model is meshed with an increasing number of SHELL281 elements until there is seen convergence in the structural error; this is seen in Figure 62.

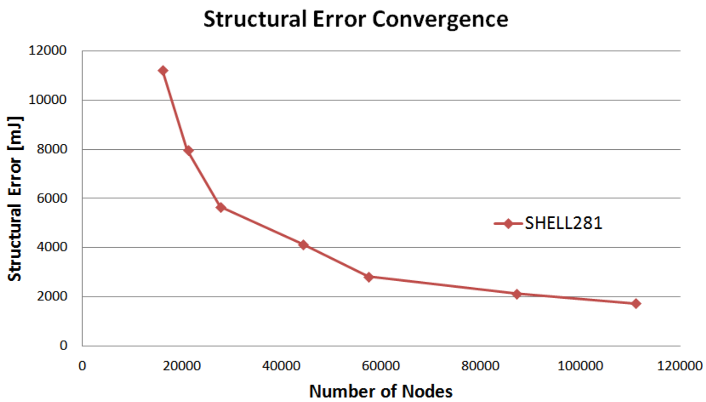

Figure 62: Convergence of structural error in the lifeboat support structure

The meshing of the structure is accepted from the structural error convergence with 36518 elements corresponding to 110944 nodes. The final maximum face size of the mesh is 35 mm and can be seen in Figure 63. The beam analyzed for shear lag has a flange width of 300 mm, and Ansys uses 8 structural elements in the width of the flange.

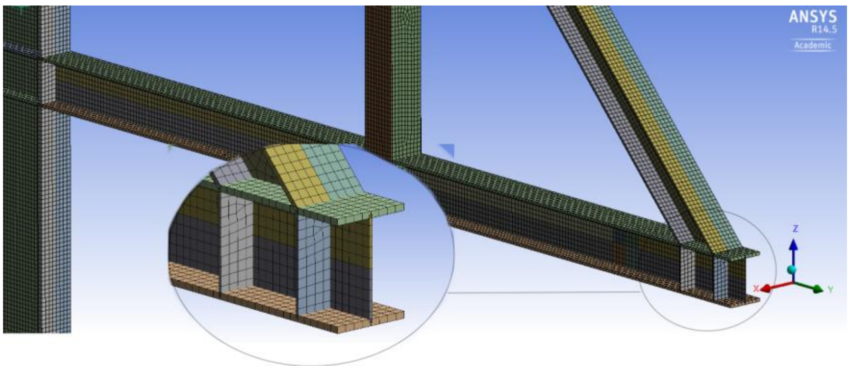

Figure 63: Mesh in Ansys model, the model is meshed with shell element and added a thickness

The vertical *beam 1* is fixed at the bottom for all degrees of freedom, and at the top *beam 1* is supported with a displacement support = 0 in the x- and y-directions, as also described for the ROSA model. To check that the support is implemented as intended in the model, the force reaction at the top of *beam 1* is checked. Also the deformation figure is checked. The reaction in the top of *beam 1* is -1.016e-3 N or almost zero in the x-direction and -979 kN in the y-direction, and no forces in the z-direction.

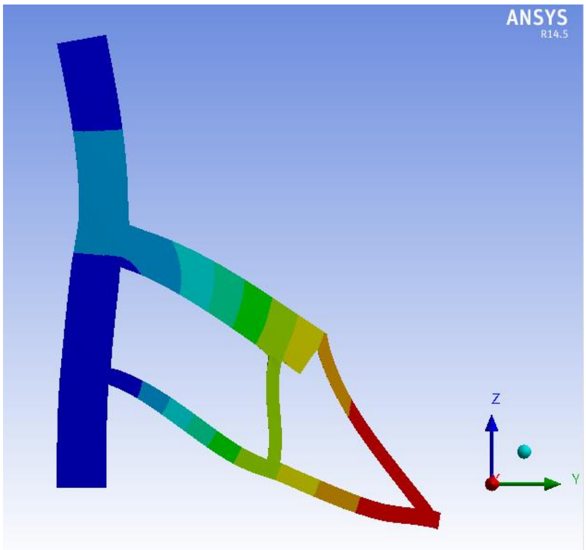

Figure 64: Deformation of the model scaled 71 times

From the deformation in Figure 64 it is seen that the top of the beam is free to rotate around the x-axis, and that the bottom is fixed for rotation, so the boundary conditions are accepted.

The "Standard Earth Gravity" function in Ansys is applied to the structure. The uniformly distributed load of 20 kN/m is applied in the Ansys model by using the "Line Pressure" function. The distributed load is applied to the center of *beam 3* as seen in Figure 65.

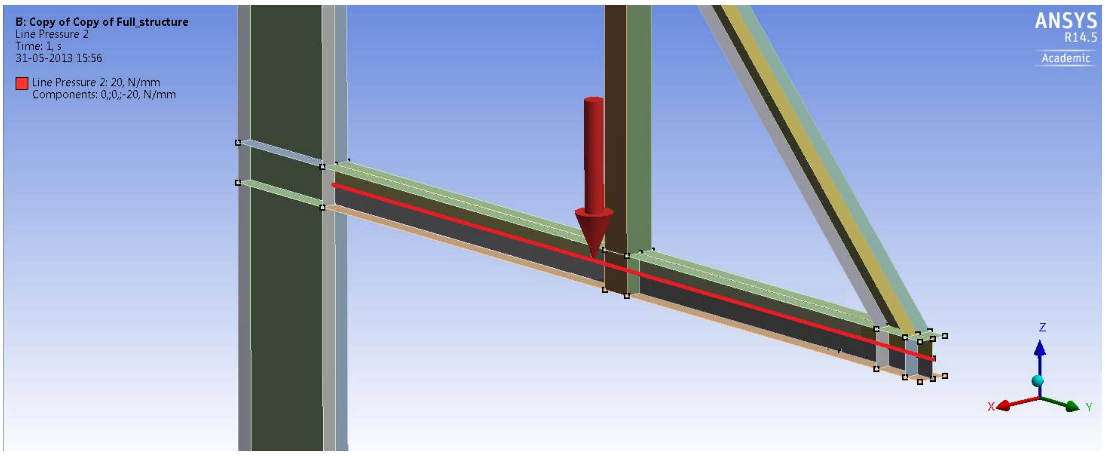

Figure 65: Uniformly distributed line load applied to the center of *beam 3*

The point loads in point 1, 2 and 3 are applied to the web of *beam 3* in its full height, as seen in Figure 66. The horizontal load of 600 kN is applied 290 mm above the beam center in the ROSA model. In the Ansys model this load is applied to the center of the web and a moment of 600 kN·0.29 m = 174 kNm is added. This moment is applied on the web on a square of 300 mm times 300 mm as seen below.

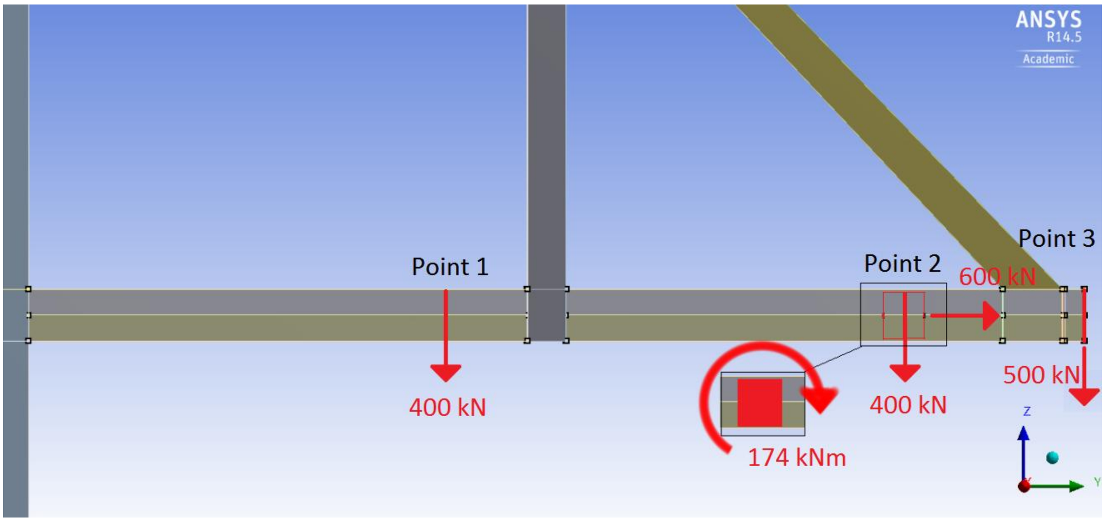

Figure 66: Point loads and moment

With the loads applied as described above the maximum directional displacement in the right end of *beam 3* is compared with the ROSA model. In the ROSA model the displacement in z-direction in the end node was -47.98 mm and in the Ansys model the displacement is -50.96 mm or 5.8% more which is assessed to be acceptable.

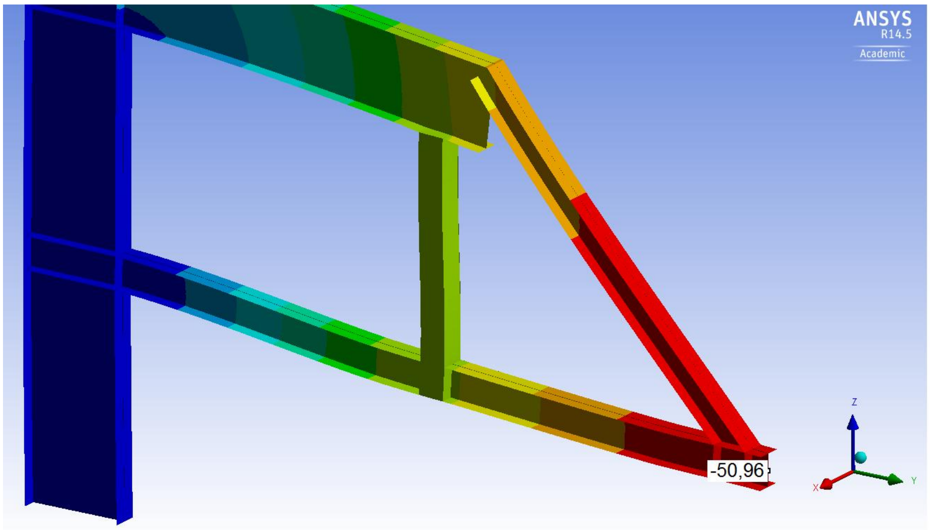

Figure 67: Displacement in the right end of *beam 3* is -50.96 mm, or 5.8% more than in the ROSA model

5.3.1. Effective width calculated from Ansys model

In the Ansys model the β-values has been calculated as described earlier in section 2.2.1 but β was raised to the power of κ (β^{κ}) to allow elastic-plastic shear deformation in the web-flange joint as explained in Eq. 5.1. For comparison the calculations has been performed in the same points as done in STRECH.

In the Ansys model the β-values has been checked both in the top flange and in the bottom flange calculated from the element stresses. The difference in the two flanges is less than 1.25 % for the first 16 points, and only in the last 5 points a bigger difference is seen, with the largest difference of 6.8 %. The smallest β-values are found in the top flange, why this flange is used as reference for the β-values calculated from the Ansys model.

The β-values calculated from the Ansys model in *beam 3* can be seen in Figure 68.

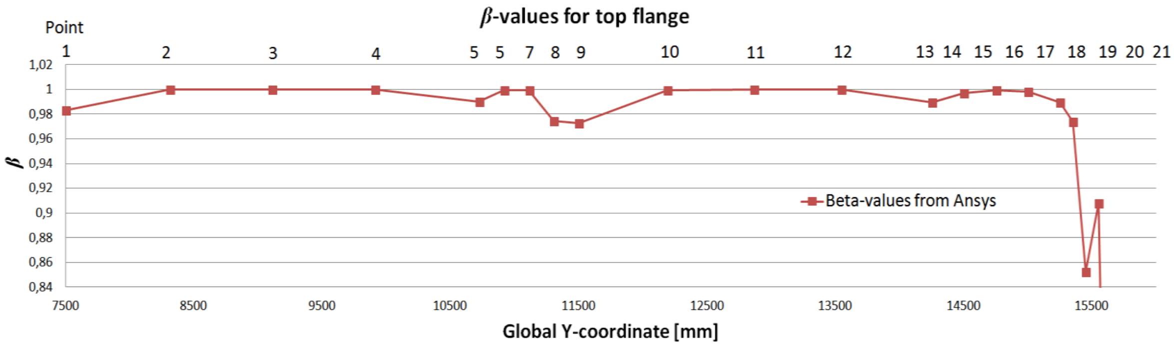

Figure 68: β-values calculated from Ansys model for *beam 3*, X-axis is the global beam axis

The β-value for the last point is 0.39 and is not seen on the graph. The stresses in this point are very small, from -2 MPa to 6 MPa, and the calculated β-value here is not of interest in the comparison with the values calculated by STRECH. In the beam-end the moment is zero or very close to zero, but as a large vertical load is acting in the web right at the beam-end, this leads to large shear stresses, and consequently to the small β-value right at the beam-end, as also described in section 2.2.1. The Ansys Workbench files used in this section can be found in App. (7).

5.4. Comparison of β-values from STRECH and from Ansys

The effect of shear lag in a lifeboat support structure, designed for an offshore platform, has in the previous been analyzed. The structure has been analyzed both by the ROSAP software and by Ansys Workbench. In ROSAP the structure was modeled with beam elements, and the effects of shear lag was determined by the method described in [2]. In Ansys the structure was modeled with 8-noded shell elements, and the β-value was determined by Eq. 2.10. The calculated flange width reduction factors from the two methods will be compared in this section.

One beam in the analyzed structure has been checked for shear lag, and the moment curve calculated by ROSA for this beam is repeated below. When a reduction of the flange width is performed it will change the effective stiffness of the beam, which again will change the moment distribution in the beam. This changed moment distribution is not calculated in ROSAP. STRECH uses the reduced flange widths to calculate new moments of inertia in the stress points and the unchanged moment distribution when the stresses are calculated. The β-values calculated by STRECH allow elastic-plastic shear deformation in the web-flange joint by β^{κ}. κ expresses the ratio b_0/L_e for a flange without longitudinal stiffeners.

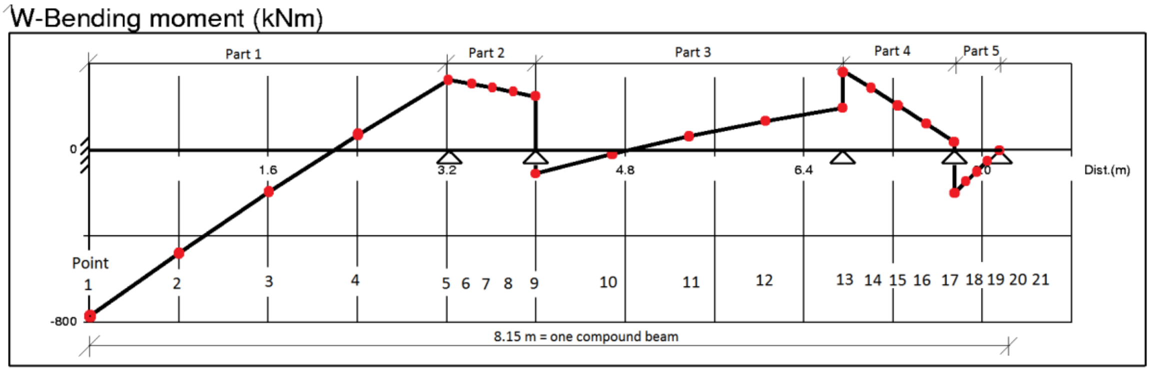

Figure 69: Bending moment curve for the analyzed beam, five beams in one compound beam

In Ansys a linear analysis was performed and the calculated β-values were raised to the power of the same κ-values as done in STRECH to allow elastic-plastic shear deformation. By doing so the β-values should be fully comparable between the two models. The calculated β-values are compared in the graphs below.

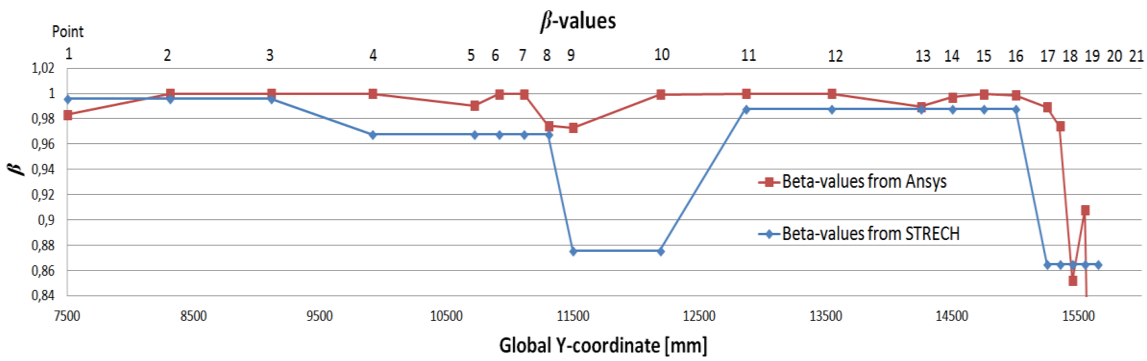

Figure 70: β-values calculated from STRECH and Ansys compared along *beam 3*

From the comparison of β-values in Figure 70 it is seen that for most points STRECH is doing a conservative calculation of the flange width reduction. From section 5.1.1 it is known that STRECH chooses the minimum β-value, equivalent to a *hogging* moment curve. The moment curve for *beam 3* is more linear than expressing *hogging*- or *sagging*-bending. In [2] no formula is given for a linear moment curve, but Eq. 3.10 suggests such a formula.

When comparing the values calculated by using the formula from [2] for *hogging* bending with *linear* bending from Eq. 3.10, and a L_e of 1.8 m, it is seen that *linear* bending is 0.7% bigger than the *hogging* value. The difference between *hogging* and *linear* bending becomes bigger with smaller L_e, with a Le = 1 m linear bending is 2.1% bigger. From this comparison it can be seen that using β for a *hogging* moment curve can be accepted with long distance between points of zero bending, but when L_e becomes shorter attention needs to be given to whether a formula for linear bending should be used. STRECH is greatly influenced by points of zero moment along the beam. It is clearly seen in point 9 and 10 on the two previous figures, here L_e is only 0.84 m and it leads to a β-value of 0.876. The percentage difference between the calculated values are listed below, where the last column describes difference divided with the Ansys value in percent.

Table 12: β-values from Ansys and STRECH respectively; the last column is (Ansys-STRECH)/Ansys in %.

Stress point	β from Ansys	β from STRECH	Difference in %
1	0.983	0.996	-1.29
2	0.999	0.996	0.40
3	0.999	0.996	0.39
4	0.999	0.968	3.19
5	0.990	0.968	2.25
6	0.999	0.968	3.15
7	0.999	0.968	3.15
8	0.975	0.968	0.67
9	0.973	0.876	9.96
10	0.999	0.876	12.33
11	0.999	0.988	1.18
12	0.999	0.988	1.20
13	0.989	0.988	0.14
14	0.997	0.988	0.90
15	0.999	0.988	1.17
16	0.998	0.988	1.05
17	0.989	0.865	12.56
18	0.974	0.865	11.20
19	0.852	0.865	-1.48
20	0.908	0.865	4.74
21	0.394	0.865	-119.03

Only in three points the Ansys analysis leads to smaller β-values than STRECH. In the first point Ansys gives a value 1.3% smaller than STRECH. As the Ansys model is expected to describe the boundary condition at the beginning of the beam quite well, the value from Ansys must be considered. This is contrary to what was expected and described in the introduction, but the difference is small, only 1.3% from the STRECH calculated value.

In point 19 the value from Ansys is also smaller than the value form STRECH. Here the difference is 1.48% and the point is located where the top flange of *beam 5* is connected to *beam 3*. It is illustrated in Figure 71.

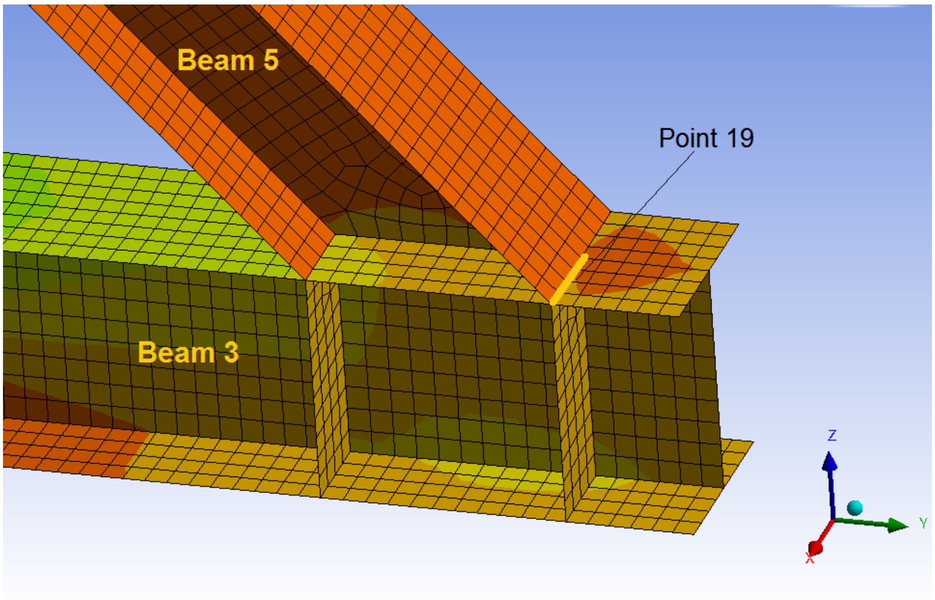

Figure 71: Point 19 gives 1.48% smaller β-value in the Ansys model; the colors describe the normal stress distribution along the beam axis of beam 3, the beam number refer to the numbers given in Figure 60

In the last point the value from Ansys is much smaller than the value from STRECH, but as already described the stresses here are very low. The small value from Ansys can be explained by the vertical force working in the web right at the beam-end, leading to large shear stresses. The method used to calculate the effective width from the shell model, does not give the correct answer when only shear stresses are present in point where the effective width is calculated. The normal stress distribution in the top flange of the shell model of beam 3 can be seen in Figure 72.

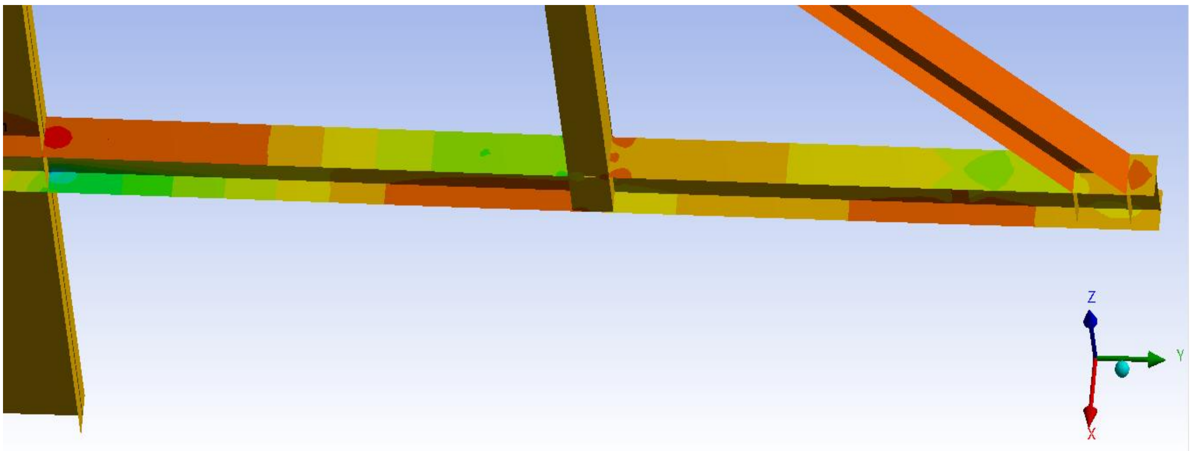

Figure 72: Averaged normal stresses in the top flange of the analyzed beam

As seen above the normal stress is much closer to a linear distribution than what was the case for the two other shell models (one span T-section in Figure 14 and three span I-section in Figure 40). As the shell model is expected to give a better description of the shear lag propagation along *beam 3* it can be seen that the flange width reduction is smaller than when the β-values are found by STRECH, making STRECH too conservative. Also it can be seen that shear lag effects are very small in the first 7 checked points in the shell model (except for the first point). This is the end of the beam which is welded to the vertical beam. From this it can be seen that when a beam is welded to an adjacent member, and the flange end is not free to deform as described in the introduction, then shear lag is not so big a problem.

6. Discussion

In section 2 the theoretical solution is based upon a continuous beam on equidistant supports with infinitely wide top-plate, but in the FE-Model made in Ansys only a one span beam with finite top-plate width is used. If the FE-Model should have been fully comparable, more than a one span beam with the 400 mm wide top-plate should have been used.

The ambition with the report from the beginning was to check both hot-rolled standard section I-beams and welded sections with similar size for shear lag. As both the theoretical solution, the solution by the standardized formulas from EC3 and the solution made by the Ramboll software were compared to a FE-Model meshed with shell elements; only sharp-edged welded sections have been checked.

The method used to calculate the effective width from the FE-Models has proved to be good when it is used for a point in a beam where normal stresses are caused by a bending moment. On the other hand it was found that when the same method was used for a point where the moment was zero and large shear stresses were present; this method could not be used and could lead to a negative reduction factor. A negative reduction factor is equivalent to a negative flange width and does not have any physical interpretation, why these small or negative flange widths have not been given attention in the report.

7. Conclusion

When a transverse loaded beam is checked for shear lag according to EC3, the moment curve is used to identify how much the flange width should be reduced. The highest reduction is when the moment curve expresses hogging bending, that would be e.g. over an internal support. Reactions from a support lead to a concentration of shear stresses, and it was found that the presences of shear stresses are the driving factor for shear lag. Shear stresses can also be seen as a change in the direction for the principal stresses, and this leads to a high reduction of the effective width. It can be concluded that shear stresses controls the amount of shear lag in a beam, and large shear stresses can be identified on the moment curve as hogging bending in a continuous beam. If the beam is simply supported at the end the moment is zero, but large shear stresses can be present, and reduce the effective flange width.

It is expected that the propagation of shear lag would be different if a beam is welded to an adjacent beam at the beam-end and not simply supported. This would activate the flange in its full width right from the start of the beam. It is seen in a FE-Model with shell elements that the effect of shear lag in this situation is less than when a beam is simply supported.

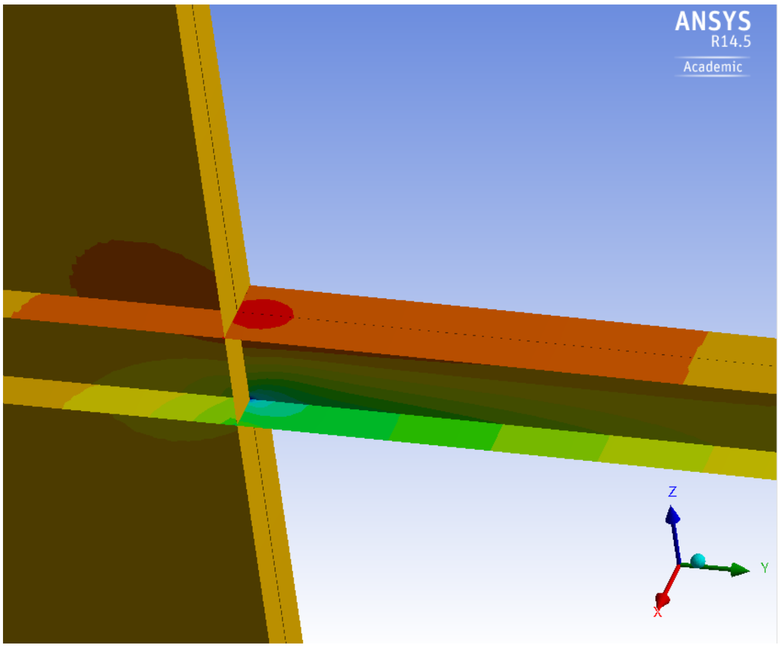

Figure 73: Normal stress in the y-direction, the vertical beam is checked for effects of shear lag

In a FE-Model the checked beam is attached to an I-section beam as seen above. The webs of the two beams are coinciding, leading to a higher stiffness than at the flange edges. As high stiffness attracts stresses it can be seen from the beam normal stresses in the y-direction, that they are greater where the webs are connected. This leads to a bigger reduction factor for the flange width at the beam start. As there is a bending moment in the horizontal beam where it is attached to the vertical beam, the situation here can also be described as a point of hogging bending. When the reduction factor is calculated by the formula for hogging bending from [2] and compared with the FE-Model it is seen in Table 12 that the reduction factor calculated from the FE-Model is 1.29% smaller than when the formula for hogging bending is used, (can also be seen in Point 1 in Figure 75). It can be concluded that the effects of shear lag is different when a beam is attached to an adjacent beam, but the situation has to be analyzed carefully. The normal stress further along the beam is close to linear which means that there is no shear lag effect. This can also be seen for the mentioned beam in Table 12.

EC3 opens a question whether shear lag has to be included in rolled standard sections and beams with similar size. This has been checked in a beam with similar size as a HE400B but without the rounding radii's. The beam is part of a structure assessed by Ramboll Oil & Gas for a lifeboat support (the same as seen in Figure 73). The beam has been modeled in a FE program and meshed with shell elements. The flange width reduction factor has been calculated in 21 points along the beam. The results are seen below.

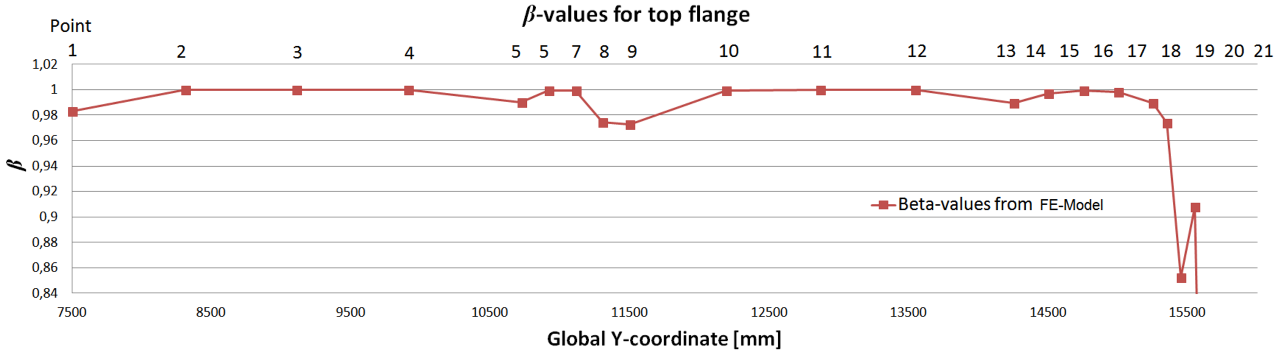

Figure 74: Flange width reduction factors calculated in 21 points along a welded I-section beam with similar size as a HE400B in a shell model

Except from the last 3 points (last point is not seen on the graph) the β-values expresses the reduction of the flange width that should be performed because of shear lag. The small β-values in the last 3 points is not representative and have to be explained by large shear stresses in the beam-end and the method used to calculate the β-value from the shell model. In point 8, 9 and 18 where the largest reduction is calculated the flange width has to be reduced by approximately 2.5 %. This concludes that the effects of shear lag is not big but have to be included when the load bearing capacity of a standard I-section beam is calculated. The effect of shear lag will in this situation lead to higher stresses and a larger deflection of the beam than what would be calculated if classical beam theory was used.

The beam checked for shear lag in Figure 74 was assessed with inclusion of shear lag effects according to [2] by Ramboll's in-house software (STRECH). This led to large reductions of the flange width and therefore a reduction of the load bearing capacity. These reduction factors (β-values) are seen compared with the reduction factors calculated from the shell model in Figure 75.

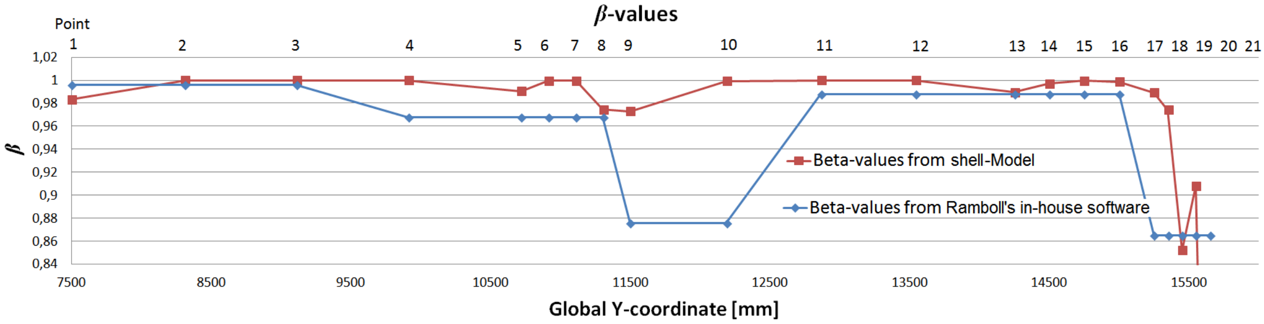

Figure 75: Comparison of β-values calculated from shell-model and Rambool's in-house software "STRECH"

From Figure 75 it can be seen that the β-values calculated by STRECH for this load case are larger. The flange width should be reduced 12.4% at point 9 and 10 according to STRECH. This is 9.96% and 12.33% more than the values from the shell-model for the two points respectively. The β-values in points 17 - 21 calculated by STRECH are also small. Here the flange width should be reduced by13.5%. Comparing with the reduction calculated from the shell-model in point 17 and 18 it is 12.56% and 11.20% higher reduction respectively. In this case it is clear that the effect of shear lag calculated by STRECH is overestimated, and too conservative.

List of references:

[1] DS/EN 1993-1-1; July 2007, Eurocode 3: Design of steel structures – Part 1-1: General rules and rules for buildings.

[2] DS/EN 1993-1-5; October 2006, Eurocode 3: Design of Steel structures – Part 1-5: Plated structural elements.

[3] Troitsky M.S.: Stiffened Plates Bending, Stability and Vibrations. Elsevier Scientific Publishing Company. Amsterdam 1976.

[4] Timoshenko Stephen P.; Goodier J. N.: Theory of Elasticity, International edition. McGraw-Hill, Inc. 1970

[5] Damkilde Lars, maj 2008, Noter om "Tværsnitsanalyse" fra undervisning i Statik og Styrkelære.

[6] Larsen H.J.; Riberholt H.: Trækonstruktioner Beregning 3. udgave Statens Byggeforskningsinstitut 1994.

[7] G. Sedlacek et al.: Commentary and worked examples to EN 1993-1-5 “Plated structural elements”. Joint report, EUR 22898 EN – 2007

[8] G. Sedlachek et al.: A simplified Method for the Determination of the Effective Width Due to Shear Lag Effects. Institute of Steel Structures, Rheinisch-Westfälische Hochschule Aachen, Mies-van-der-Rohe-Strasse 1, D-5100 Aachen, Germany. April 1992.

[9] Cook Robert D et al.: Concepts and Applications of Finite Element Analysis. 4th ed. John Wiley & Sons. Inc. 2001.

[10] Lesson 7 of continuum mechanics by Lars Damkilde, autumn 2011.

[11] EN 1993-1-5 DK NA; November 2007, National annex to Eurocode 3: Design of steel structures – Part 1-5: Plated structural elements.

[12] DS/EN 1993-1-5/AC; May 2009, Rettelsesblad 1. udgave.